

CERTAIN X-RAY DIFFRACTION METHODS OF INVESTIGATING COLD WORKED METALS

D. M. VASIL'EV and B. I. SMIRNOV

Usp. Fiz. Nauk 73, 503-558 (March, 1961)

DURING the last few decades x-ray investigations of the structure of strained metals found wide application, and much progress was made in this field. Our literature, however, still has no systematic exposition of the basic results. The well known survey by Greenough¹ considers only papers published prior to 1951, and has become rather obsolete by now. The survey papers presented by Barrett and Guinier at the Detroit Conference² treat many problems quite briefly.

The present review is devoted essentially to distortions in the structure of plastically deformed (cold worked) metals, which manifest themselves as changes in the positions of x-ray diffraction lines and in the forms, widths and integrated intensities of these lines. However, since microstresses are frequently investigated by methods originally developed for the study of macrostresses produced by macroelastic loading, we shall consider briefly these methods, too.

We do not discuss in this survey various methods used to study the mosaic structure and its influence on metal properties, since this problem was recently considered by Hirsch.³ In addition, we felt that we could dispense with a detailed description of the harmonic analysis of the profile of a diffraction line, since this was done by Warren in his survey;⁴ we stopped only to discuss a few principal problems in this procedure, which are of importance in practical measurements.

1. SHIFT OF X-RAY DIFFRACTION LINES IN MACROELASTIC DEFORMATIONS

From the Bragg equation

$$2d \sin \theta = \lambda, \tag{1.1}$$

where λ is the wavelength, we see that a change in the distance d between planes causes a change in the diffraction angle θ , i.e., a shift in the x-ray line. The possible use of this fact was first pointed out by Ioffe and Kirpicheva,⁵ who proposed to determine the elastic constants of single crystals by measuring the lattice constant of a loaded sample.

Lester and Aborn⁶ have found that in a stretched thin steel specimen the distances between planes perpendicular to the specimen axis increase linearly with increasing applied stress.

Aksenov⁷ considered in general form the variation of the shape of a diffraction ring for linear and volume stresses, with allowance for the anisotropy of the crystallites in a polycrystalline sample. However, in spite of the valuable results obtained by Aksenov, the un-

wieldy mathematical formalism of the theory makes practical use of the derived formulas extremely difficult.

Sachs and Weerts⁸ used flat film and large diffraction angles. They showed that the stress σ_r in a loaded duraluminum specimen as determined by x-ray diffraction is directly proportional to the stress σ_m , determined by the usual "mechanical" means. A deviation from direct proportionality is observed only after the macroscopic yield point is reached.

Wever and Moller⁹ gave a formula for the sum of the principal stresses

$$\sigma_1 + \sigma_2 = - \frac{E}{\mu} \frac{d_{\perp} - d_0}{d_0}, \tag{1.2}$$

where E and μ are the known elastic constants, while d_{\perp} and d_0 are the interplanar spacings for planes parallel to the specimen axis in the loaded and unloaded states, respectively. Using a standard substance, the authors obtained an accuracy of ± 6 kg/mm² for steel specimens. They, and also the authors of references 10 and 11, noted the existence of a direct proportionality between σ_r and σ_m .

Barrett and Gensamer¹² described a method for determining σ_1 and σ_2 separately from their known directions and the known d_0 . Glocker and Osswald¹³ devised a method for determining the magnitudes and directions of σ_1 and σ_2 for known d_0 . It was shown later¹⁴ that angle photographs yield the magnitudes and directions of σ_1 and σ_2 without knowledge of d_0 .

The most general formula for the normal stress σ_{φ} , acting in a direction φ parallel to the surface, was given by Glocker, Hess, and Schaaber¹⁵

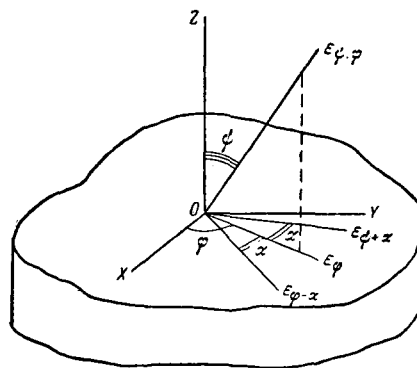


FIG. 1. Measurement of stresses by the method of angle photographs; $\epsilon_{\psi, \varphi}$ - relative change of the interplanar distances $\Delta d/d$ in the direction ψ, φ measured from the changes in the positions of the diffraction lines.

$$\sigma_{\varphi} = \frac{E}{1+\mu} \frac{\epsilon_{\psi_2, \varphi} - \epsilon_{\psi_1, \varphi}}{\sin^2 \psi_2 - \sin^2 \psi_1} \quad (1.3)$$

Here ψ and φ are the polar distance and the azimuth of the direction along which the deformation is measured (Fig. 1). Here

$$\epsilon_{\psi_2, \varphi} - \epsilon_{\psi_1, \varphi} \approx \frac{\epsilon_{\psi_2, \varphi} - \epsilon_{\psi_1, \varphi}}{d_{\psi_1, \varphi}} \quad (1.4)$$

Formula (1.4) makes it possible to determine σ_{φ} from a single "oblique" photograph, for with $\psi_0 \neq 0$ a single x-ray picture yields the values of the strains $\epsilon_{\psi_2, \varphi}$ and $\epsilon_{\psi_1, \varphi}$ corresponding to the directions $\psi_2 = \psi_0 + \eta$ and $\psi_1 = \psi_0 - \eta$, where $\eta = 90^\circ - \beta$.

Glocker's group¹⁶ has developed an expedient procedure for the determination of σ_{φ} , using photographs with a standard substance with known parameter. If the standard line is obtained at a smaller diffraction angle than the specimen line, and a flat film at an angle $\psi_0 = 45^\circ$ is employed, the formula used is

$$\sigma_{\varphi} = (\Delta_{-} - \Delta_{+}) C_{+-} \quad (1.5)$$

Here Δ_{\mp} are the distances from the standard line to the specimen line on the side of the film where $\psi = 45^\circ \mp \eta$, respectively, while C_{+-} is a constant that depends on the wavelength, the parameter of the standard, and the distance from the specimen to the film. The value of $\sigma_1 + \sigma_2$ is given by

$$-(\sigma_1 + \sigma_2) = (\Delta_0 - \Delta_{\perp}) C_{\perp 0} \quad (1.6)$$

where Δ_0 is the distance from the standard line to the specimen line in the unstressed state, Δ_{\perp} is the analogous distance in the stressed state for $\psi_0 = 0^\circ$, and $C_{\perp 0}$ is a constant analogous to C_{+-} .

Fuks¹⁷ proposed the use of nomograms for photographs of steel specimens with a silver standard.

Vasil'ev and Vashchenko¹⁸ gave for back-reflection pictures on a flat film a formula which does not call for the knowledge of the parameter of the standard substance

$$\frac{\Delta d}{d} = \cos^2 \theta \cdot \cos(180^\circ - 2\theta) \left(\frac{l_2 - l_1}{l_1} - \frac{l_{20} - l_{10}}{l_{10}} \right) \quad (1.7)$$

Here l_1 and l_2 are the distances from the center of the x-ray diffraction pattern to the sample line, corresponding to two states of the specimen, 1 and 2; l_{1S} and l_{2S} are the same distances for the standard substance. For angle pictures, in the case when it becomes necessary to determine l separately for the sides $\psi_0 + \eta$ and $\psi_0 - \eta$, Vasil'ev¹⁹ proposed the use of a reference located at a fixed distance from the center of the x-ray diffraction picture.

To determine the magnitudes and directions of the principal stresses it is necessary, according to Gisen, Glocker, and Osswald,¹⁴ to take angle pictures at constant ψ_0 and at azimuths φ , $\varphi + 90^\circ$ and $\varphi \pm \alpha$. Another procedure calls for pictures with azimuths φ , $\varphi + \alpha$, and $\varphi - \alpha$ (see Fig. 1). The method of determining σ_1 and σ_2 from one oblique picture²¹ has not found practical application because of its low accu-

racy (± 6 kg/mm²), whereas a procedure involving three or four oblique pictures gives an accuracy²² ± 2 kg/mm², and even²³ 0.5 kg/mm².

It was assumed in the cited investigations that the stress σ_{\perp} perpendicular to the surface is zero. Actually, however, the effective depth of penetration of the customarily used x-rays is several hundredths of a millimeter,^{24,25} so that σ_{\perp} can no longer be assumed as equal to zero at all times in the presence of large strain gradients along the normal to the surface. This question was first considered by Kurdyumov and his co-workers,²⁶ and Romberg²⁷ gave formulas corresponding to a tri-axial stressed state. Investigating hardened steel cylinders in cobalt radiation, the authors of reference 26 concluded that σ_{\perp} does not influence the positions of the x-ray lines, and the line shift due to going from long to short cylinders is caused by the "edge effect." An analysis of the "edge effect" for the plane problem was given by Vasil'ev and Tsobkallo.²⁸ Schaaber,²⁹ using an aluminum alloy and copper radiation, detected a noticeable influence of the stress perpendicular to the surface on the positions of the x-ray lines.

In the presence of a tri-axial stressed state it is necessary to employ the formula¹⁹

$$\sigma_{\varphi} - k\sigma_{\perp} = \frac{E}{1+\mu} \frac{\epsilon_{\psi_2, \varphi} - \epsilon_{\psi_1, \varphi}}{\sin^2 \psi_2 - \sin^2 \psi_1} \quad (1.8)$$

where σ_{\perp} is the stress perpendicular to the surface, and k is a coefficient that takes into account the effect of σ_{\perp} on the positions of the x-ray lines and depends on the relation between the effective depth of penetration of the x-rays and the dimensions of the area within which σ_{\perp} changes from zero to its maximum value, corresponding to the deep layers of the specimen.

If the formulas used contain d_0 and the x-ray lines of the specimen in the stressed state are broadened, it becomes necessary to take into account the interaction between the closely located components of the $K\alpha$ doublet.^{18,30-32} If the line broadening is large, the shift of the maximum of the x-ray line reaches one-third of the distance between the components of the doublet, equivalent in terms of stress to a systematic error¹⁸ on the order of 50 kg/mm² for steel in cobalt radiation.

As noted earlier, a direct proportionality between σ_R and σ_M was observed even in the early investigations.⁸⁻¹¹ However, as was shown by Moller and Barbers,³³ the calculation of σ_R from the mechanically-measured elastic constants E_M and μ_M leads to a difference between σ_R and σ_M . The authors have attributed this to the fact that in the tests for E_M and μ_M the specimen behaves like a quasi-isotropic specimen, while the photograph and diffraction pattern are produced only by crystallites oriented in a definite manner, so that to calculate σ_R it is necessary to assume values of E_R and μ_R corresponding to the reflecting planes. Using "Armco" iron, they found that

$$\left(\frac{\mu}{E}\right)_r \approx 1.2 \left(\frac{\mu}{E}\right)_m \quad (1.9)$$

Moller and Strunk³⁴ compared the ratio E_r/E_m obtained for steel in cobalt $K\alpha$ radiation with the values obtained by Voigt³⁵ and found no agreement between the experimental and the calculated data.

Rovinskii^{36,37} determined in a series of investigations the ratio σ_r/σ_m , assuming it to be equal to the ratio of the experimentally measured strains ϵ_r/ϵ_m . For steel with 0.23 percent carbon this ratio, in cobalt $K\alpha$ radiation, was found to be 0.40–1.64 for coarse and fine grain states respectively. He assumed that the difference between the x-ray elastic characteristics and the mechanical ones may be due not only to anisotropy, but also to inhomogeneity of the structure, caused by the presence of inclusions with elastic constants other than that of the main substance, and by the presence of intercrystallite layers, as well as to the influence of the mosaic structure, which prevents the transmission of external forces to the lattice.

The difference between E_r or μ_r and E_m or μ_s can be investigated in greater detail by determining not the ratio μ/E , but each of the constants separately, which can be done by angle pictures with great accuracy.³⁸

According to Voigt,³⁵ the strain in each grain of a polycrystalline material is the same and is equal to the macroscopic strain, while the stresses in the different grains differ from each other. The average stress, equal to the applied stress σ_m , is calculated by summing over the differently-oriented grains, and then the values of the elastic constants E_ϵ and μ_ϵ are independent of the indices (hkl) of the reflecting plane. According to Reuss,³⁹ to the contrary, the stresses acting on all the grains are assumed to be the same and equal to σ_m , while the strains in each grain depend on the grain orientation. Then E_σ and μ_σ will depend on the (hkl) indices.

Moller and Martin⁴⁰ compared the experimentally obtained values of E_{310} and μ_{310} of steel specimens with the values of E and μ calculated after Voigt and Reuss, and found no agreement between the experimental and calculated values. The authors recommend that the values of E_r and μ_r determined directly from experiment be used for x-ray measurements. Neerfeld⁴¹ found, for steel samples and cobalt and chromium $K\alpha$ radiation, that the use of E_r and μ_r in the form

$$E_r = \frac{E_\epsilon + E_\sigma}{2}, \quad (1.10)$$

$$\mu_r = \frac{\mu_\epsilon + \mu_\sigma}{2} \quad (1.11)$$

yields values that agree with experiment. A similar conclusion was reached in references 42–44. The values of E_r and μ_r were calculated by Neerfeld's method for a series of materials.³² Hauk and Hummel,⁴⁵ and also Moller and Brasse,⁴⁶ propose for E_r and μ_r of an iron polycrystalline specimen the formulas

$$E_r = \frac{2E_\epsilon + E_\sigma}{3}, \quad (1.12)$$

$$\mu_r = \frac{2\mu_\epsilon + \mu_\sigma}{3}. \quad (1.13)$$

Apparently the true value of E_r lies between E_ϵ and E_σ and the true value of μ_r between μ_ϵ and μ_σ . An establishment of an exact relation between the Voigt and Reuss values of the elastic constants and the actual experimental values is of great importance to the clarification of the character of the distribution of the stresses and strains in an elastically-stressed polycrystalline specimen. If the emphasis is on the purely practical problem of determining the macroscopic stresses with the aid of x-rays, then the use of the elastic constants calculated, say, from the simplest relations (1.10) and (1.11) produces a relative error in the modulus of elasticity not more than $\pm(E_\epsilon - E_\sigma)/(E_\epsilon + E_\sigma)$, which is quite satisfactory for many practical purposes.

2. SHIFT OF X-RAY DIFFRACTION LINES IN THE REGION OF MACROPLASTIC DEFORMATIONS

The experiments described in the preceding section have shown that proportionality between the macroscopic stress σ_m and the stress σ_r determined by x-ray means is retained in the macroelastic region. If the elastic constants E_r and μ_r are suitably chosen, the following relation will hold

$$\sigma_m = \sigma_r. \quad (2.1)$$

Since the plastic shear deformation should not change, on the average, the parameters of the elementary cell inside the individual crystal layers separated by the glide planes, either direct proportionality or the fulfillment of Eq. (2.1) are expected also in the macroplastic region.

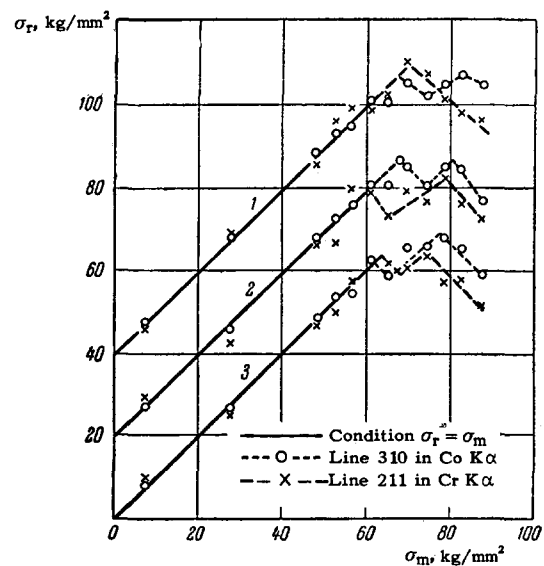


FIG. 2. Relation between σ_r and σ_m , obtained in bending of a steel specimen.⁴¹ Lines 1 and 2 are shifted vertically by 20 and 40 kg/mm²; measurements 1, 2, and 3 correspond to different portions of the specimen.

However, the very first measurements of the stresses in the macroplastic region have disclosed a deviation from relation (2.1) (Fig. 2), and in all cases the inequality $\sigma_r < \sigma_m$ was obtained on going through the macroscopic yield point σ_s . Such results were obtained in bending of duraluminum⁸ and steel specimens.^{11,33} The authors have attributed the violation of relation (2.1) to the start of plastic deformation, without discussing the mechanism of the phenomenon itself.

Bollenrath, Hauk, and Osswald⁴⁷ measured the stresses σ_r produced by stretching steel specimens under load, and the residual stresses after macro-unloading. They established that when $\sigma_m = \sigma_s$ the value of σ_r decreases sharply and continues to decrease with further increase in the degree of plastic deformation, in spite of the increase in σ_m . After macro-unloading, residual axial compression stresses were observed on the surface of the specimen. Successive etching of layers on the unloaded specimen have shown that axial and transverse tension stresses appear in the deeper layers of the specimen, and the outer zone of the specimen, which is under the influence of the residual compression stresses, extends deep enough to make its area approximately one-half the area of the cross section of the specimen. The authors attribute their results to the fact that the crystallites located on the surface of the specimen have more degrees of freedom in plastic deformation and therefore have less resistance to deformation than those located deeper. These outer layers are underloaded and the internal ones overloaded compared with the macroscopic stress σ_m , so that after macro-unloading axial compression stresses occur in the outer layers, while axial tension forces appear in the internal layers. In a later work,⁴⁸ a decrease in σ_r on passing through the yield point was observed also under compression.

It is interesting to note that even Heyn⁴⁹ observed in a stretched steel specimen a pattern of residual strains, analogous to that obtained in reference 47, but explained its origin in a different manner. He assumed that a thin outer layer of the specimen, ≈ 0.1 mm thick, plays the role of a "rigid shell" through which the forces are transmitted from the heads to the remaining part of the specimen. This "rigid shell" is overloaded when tension is applied, and its strain will be greater than average, so that a compressive stress results after unloading.

Glocker and Hasenmeier⁵⁰ observed that in cobalt $K\alpha$ radiation the deviation of σ_r from σ_m is observed in steel only after the yield point is reached, whereas if the softer chromium $K\alpha$ radiation is used, this deviation occurs already at $(0.5 - 0.7) \sigma_s$. The authors have assumed that their results are a confirmation of the existence of a weakened surface layer, extending to a depth commensurate with the effective depth of penetration of the chromium $K\alpha$ radiation, i.e., on the order of 0.01 mm. In the mentioned references

47, 48, and 50, a procedure of perpendicular photographs was used from the side surface of the specimen under load, and it was assumed that the strains measured with the aid of the x-rays can be converted into stresses σ_r by means of formula (1.2).

Wood proposed at first a different explanation for this problem. He observed⁵¹ a residual change in the parameter in rolled copper specimens exposed at right angles, and related the change with the absorption of energy during deformation. Later on Wood observed analogous changes on rolled specimens of α -brass,⁵² silver, copper, nickel, aluminum, and molybdenum.⁵³ The results with α -brass were attributed to the fact that the lattice of this substance is no longer cubic after it is rolled, and the explanation for other materials was that the rolling produces a "broadening" of the lattice, which leads to a reduction in its stability. These investigations were objected to by Rovinskii,⁵⁴ who showed that no change in the residual parameter is observed on cold-hardened copper powders, so that the described effects could be due to the influence of the residual macrostresses produced during rolling.

Wood and Smith⁵⁵ investigated the changes in the interplanar distances, for the (310) planes of an iron specimen in simple tension. The relative change in interplanar distance, $\Delta d/d = \epsilon_r^\perp$, between planes almost parallel to the lateral surface of the specimen (in right-angle photography), was plotted as a function of the applied stress σ_m (Fig. 3). The dependence $\sigma_m = \varphi(\epsilon_r^\perp)$ was called by the author the "strain diagram of the atomic lattice." In subsequent investigations Wood and Smith obtained similar relationships for copper,⁵⁶ iron,⁵⁷ aluminum,⁵⁸ and soft steel.⁵⁹ The

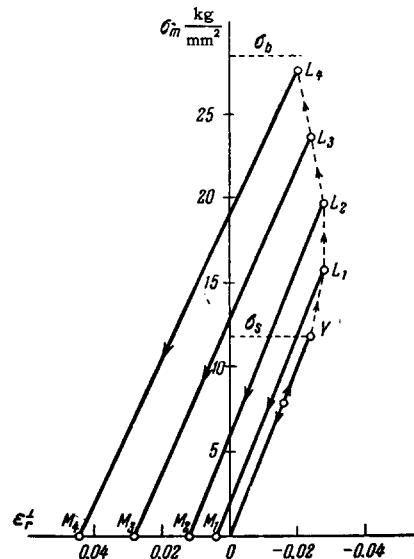


FIG. 3. Diagram⁵⁵ of the deformation $\sigma_m = \varphi(\epsilon_r^\perp)$ obtained with Co $K\alpha$ radiation along the 310 direction when tension is applied to a still specimen. The unloading from the points L_1, L_2, \dots takes place along straight lines parallel to the elastic portion of the load curve. The points M_1, M_2, \dots correspond to the residual microdeformation observed in the specimen after macro-unloading.

dependence $\sigma_m = \varphi(\epsilon_F^{\perp})$ had the same character in all cases (Fig. 3). The authors have attributed⁵⁸ the observed phenomena to the fact that the lattice can experience not only the usual elastic strain, but also residual strain, which appears when $\sigma_m > \sigma_S$, and which has a sign opposite to the sign of the macroscopic deformation, in which the "reaction" of the lattice to the action of the external forces manifests itself.

Smith and Wood,⁶⁰ using specimens of soft steel, have investigated the dependence of $\Delta d/d$ on the angle between the axis of the specimen and the normal to the (310) plane. This dependence was found to correspond to the presence of residual axial compressive strains in the unloaded specimen. Thus, the authors have ultimately reached the same conclusion as other investigators,⁴⁷ that residual axial compressive strains are produced in a sample after cold-work stretching. Smith and Wood, however, believe these stresses to be due not to the influence of the weakened layer, but to the difference in resistance to deformation between the boundary regions and the internal parts of the grains. In plastic deformation the boundary regions have a higher elastic limit and are subject to higher stresses than the internal parts of the grains. After macro-unloading, the boundary regions are subjected to residual strains of the same sign as the macrostresses applied to the specimen, while the internal parts of the grains are under the influence of residual strains of opposite sign. The material of the boundaries is so highly distorted that it does not participate in the creation of x-ray diffraction lines corresponding to the coherent part of the scattering. Obviously, these residual strains are microstrains by nature.

Wood⁶¹ again investigated the dependence $\sigma_m = \varphi(\epsilon_F^{\perp})$ using specimens of soft steel in cobalt and chromium $K\alpha$ radiation, and observed after prior stretching both axial and transverse compression microstresses. He found that in cobalt $K\alpha$ radiation the x-ray yield point "coincides" with σ_S , whereas in chromium $K\alpha$ radiation it is even higher than σ_S , thus contradicting reference 50.

Greenough⁶² offered a different treatment of the residual change in interplanar spacing observed in simple stretching. He proposed that the changes are due to usual residual Heyn-Masing microstresses, i.e., microstresses due to the difference in resistance to plastic deformation between individual grains of a polycrystalline specimen (residual stresses of the second kind). Greenough pointed out that the diffraction of x-rays is selective. Actually, the diffraction pattern is produced every time not by all the crystallites in the irradiated volume, but only by those whose orientation satisfies the diffraction equation. As a result, lines with different $hk\ell$ indices, corresponding to differently oriented crystallites under microstresses of opposite signs can shift in different directions. It becomes necessary in practice to work with different radiations in order to obtain lines with different $hk\ell$ in a specified range of diffraction angles.

Consequently, if Wood's point of view⁶⁰ is correct, x-ray lines with different $hk\ell$ should give $\Delta d/d$ of only one sign; according to Greenough, however, some of the lines yield $\Delta d/d > 0$ and others $\Delta d/d < 0$. Greenough calculated the relative change in the distances between planes parallel to the specimen axis, which should be observed in metals with face-centered cubic lattice after cold-work stretching. He found that the lines 311, 400, 420, and 511/333 should yield $\Delta d/d > 0$, while the lines 222, 331, and 422 should give $\Delta d/d < 0$. He suggested that his experimental results⁶² on aluminum, copper, and nickel are in satisfactory agreement with the calculations.

Thus, if we introduce the concept of weak A-domains, which are under stresses lower than the macroscopic stresses σ_m in plastic deformation, and strong B-domains, on which stresses greater than σ_m act during deformation, then the hypotheses considered above can be briefly formulated in the following manner: 1) The hypothesis of the weakened surface layer,⁴⁷ where the A-domains are the thin surface layer of the specimen and the B-domains are the internal zone of the specimen. 2) The Heyn-Masing⁶² microstress hypothesis, where the A- and B-domains are separate grains of a polycrystalline specimen, which have acquired through different orientation less and more resistance to plastic deformation, respectively. 3) The hypothesis of near-boundary domains and internal parts of the grains.⁶⁰ The A-domains are matrix regions that participate in the creation of the diffraction pattern of coherent scattering of x-rays, while the B-domains are near-boundary zones that do not participate in the coherent scattering.

1. Generally speaking, the "weakened" surface layer can be due to the following factors: a) unaccounted for tilt of the specimen during deformation; b) uneven strength over the section of the specimen, due to technological factors (decarburization of the steel during heat treatment, different concentration of impurities over the cross section, different grain size over the cross section, etc.); c) effect of the etchant (creation of residual strains due to etching or the creation of a microrelief); d) concentration of stresses on the surface, due to the microrelief (scratches produced by a cutter, by grinding, slag inclusions, etc.); e) easier deformability of the grains on the surface ("true" weakness of the surface layer).

Production of residual strains by the etchant has been reported by Lihl,⁶³ who observed them with x-rays in steel specimens subject to chemical and electrolytic etching by various reagents. However, in a later study by Hauk, Moller, and Brasse,⁶⁴ who investigated steel specimens under widely varying etching and heat-treatment conditions, the x-ray method did not disclose any residual strains after etching. Only in the case of a very deep microrelief with irregularities on the order of 3×10^{-2} mm was a reduction in the stresses observed in a sample etched under load.

In most investigations in which the existence of a weakened surface layer was touched upon to a lesser or greater degree it is impossible to demarcate sharply the possible influence of the remaining factors. Thus, Bollenrath, Hauk, and Osswald⁴⁷ worked with steel containing 0.11 percent carbon, and the specimens were annealed in a neutral atmosphere and etched in nitric acid before testing. The same material was used in references 48 and 50, but the authors of reference 47 estimated the depth of the weakened layer to be at least 1 mm, whereas in reference 50 it is estimated to be 0.01 mm. It should be noted that the authors of reference 48 observed that recrystallization of deformed specimens leaves in the cross section two concentric zones of sharply differing grain sizes. It is possible⁷¹ that the steel used in references 47, 48, and 50 had macroinhomogeneities over the cross section from the very beginning.

Wood annealed the steel specimens in vacuum before testing. Finch⁶⁵ annealed similar specimens in either vacuum or an inert medium, with subsequent etching. Hauk⁶⁶ annealed steel specimens from iron filings and etched them later in hydrochloric and nitric acids; in no case were changes in the x-ray picture observed after deformed specimens were etched. These results contradict the data of Greenough,⁶⁷ who observed that steel specimens stretched by 11 percent and previously annealed in vacuum exhibited residual compression strains in a thin surface layer approximately 0.2 mm deep; the observations were made by electrolytic removal of the layers and radiography in cobalt, manganese, and chromium $K\alpha$ radiation.

On the basis of the simplest model of the weakened surface layer,⁴⁸ one would expect the plastic deformation under load to begin in this layer before the macroscopic yield point σ_s is reached. Such a phenomenon was observed only in the cited reference 50. In all the remaining investigations of the change in the interplanar spacing under tension^{47,60,65,68,73,74,90} it was found that the "x-ray yield point" of the surface layer coincides with σ_s . An analogous result was obtained by Glocker and Macherauch⁶⁹ in bending and torsion. Hendus and Wagner⁴² stretched specimens of steel with 0.43% carbon and observed, at stresses amounting to approximately one-half the macroscopic yield point, a jump in the x-ray deformation, with a maximum for the $CrK\alpha$ radiation, and with smaller values in cobalt and molybdenum $K\alpha$ radiation. No deviation from linearity was observed in steels containing from 0.16 to 0.76% carbon. The x-ray yield point for all steels was quite close to the macroscopic yield point σ_s .

A systematic study of the causes of residual variation in the interplanar distances after macro-homogeneous plastic deformation was made by Rovinskii and his co-workers. Having observed⁷⁰ no residual changes of the parameter in powders of "Armco" iron, copper, brass, and bronze, they have assumed that the changes in the parameter observed in solid speci-

mens are the consequence of polycrystalline structure of the specimen. Rovinskii further verified⁷¹ the hypothesis of the weakened layer, using plastically deformed steel and aluminum samples from which the core was removed. He concluded that no weakened surface layer exists, and that the effects disclosed in certain investigations were due to technological factors which play a role in the preparation and heat treatment of the specimens. He investigated in particular⁷² the behavior of surface layers of steel specimens in tension, and showed that no premature flow of these layers is observed. A similar conclusion was obtained also in reference 73. In reference 74 the effect of "slipping" was observed on some specimens, i.e., premature flow of the surface layer, depending to a great degree on the state of the surface. However, this effect is too small to influence the change in the interplanar distances. The authors believe that the particular properties of the surface layer are the consequence of mechanical working and heat treatment of the specimen.

The presence of compressive macrostresses in a thin surface layer was repeatedly investigated by known mechanical methods wherein etching of the layers changed the deflection of a flat specimen. Davidenkov and Timofeeva⁷⁵ used aluminum specimens, Glikman and Stepanov⁷⁶ steel ones, and neither observed a weakened layer in tension. In reference 77, where steel specimens were annealed under a layer of cast-iron filings prior to stretching and etched to depths up to 0.2 mm, residual compression stresses were observed at low degrees of plastic deformation, which vanished at strains on the order of several percent. The authors attribute the residual stresses not only to the "true" weakness of the surface layers, but also to the possible influence of etching.

Davidenkov, Terminasov, and Assur⁷⁸ have found in aluminum specimens residual compression stresses after tension, and x-ray and mechanical methods gave approximately similar results. Later on Davidenkov⁷⁹ concluded that in reference 78 the principal role in the creation of the "weakened" layer was played by the deep etching of the specimens prior to plastic deformation. A result analogous to that of reference 78 was obtained in reference 80. In reference 81 the mechanical method disclosed no residual strains in a surface layer of steel specimens, stretched to small degrees of plastic deformation.

2. The correctness of the Greenough hypothesis⁶² was verified in many investigations. Thus, Bateman⁸² obtained for specimens of aluminum of different degrees of purity data which did not coincide with those predicted by the Greenough hypothesis. Kappler and Reimer⁶⁸ investigated the dependence of $\Delta d/d$ on the angle β between the normal to the plane (hkl) and the axis of steel specimens, and reached the conclusion that the experimental curve agrees satisfactorily with the curve calculated after Greenough, provided

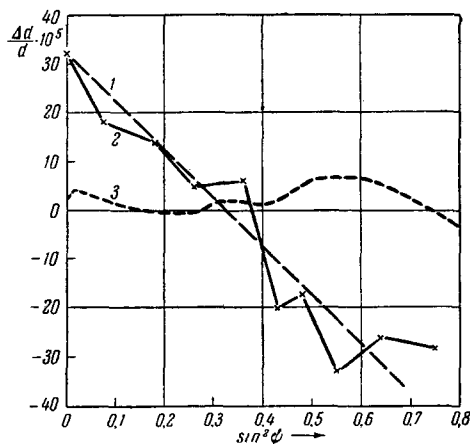


FIG. 4. Angular dependence of the relative change in the parameter, determined from the shift of the 400 line, obtained in cobalt $K\alpha$ radiation with a copper specimen stretched beforehand by 10%.⁹⁶ ψ – angle between normal to the side surface of the specimen and the normal to the (400) plane. 1 – line corresponding to the presence of axial microstress $\bar{\sigma}_{11}$; 2 – experimental points; 3 – curve calculated after Greenough.

the ordinates of the theoretical curves are increased by a factor of 7 or 8.

The angular dependence of $\Delta d/d$ was also investigated by Hauk.^{66,83} He found that the principal effect in steels and in aluminum alloys is due to the presence of the "rigid" phases Fe_3C and Al_2Cu . Superimposed on this effect is, in some specimens, a secondary effect, predicted by the Greenough hypothesis. Hauk cannot explain the reason for the angular dependence of $\Delta d/d$ in pure aluminum.

The Greenough hypothesis was also tested by Vasil'ev and Erashev.⁸⁴ They obtained a dependence of $\Delta d/d$ on the angle between the specimen axis and the (hkl) plane and reached the conclusion that the Greenough hypothesis cannot be confirmed. Since the experiments were made with small specimens cut from previously deformed large specimens, the angular dependence of $\Delta d/d$ could not be due to the influence of surface effects. Vasil'ev⁸⁵ obtained the angular dependence of $\Delta d/d$ in compressed steel specimens using $K\alpha$ radiation of cobalt, iron, chromium, and titanium. In no case was the Greenough hypothesis confirmed. Likewise, no confirmation was obtained of the Greenough hypothesis in references 89, 92, 95, 96, and 98. It should be noted that the effects observed in these investigations were approximately one order of magnitude greater than predicted by Greenough's hypothesis (Fig. 4).

3. We proceed now to discuss the third hypothesis.⁶⁰ Rovinskii,⁸⁵ analyzing the results of his own work as well as those obtained by others, concluded that this hypothesis explains the observed phenomena correctly. He assumed that in addition to "strong" grain boundaries, an analogous role is played by regions located near the slip planes. The microstresses produced by

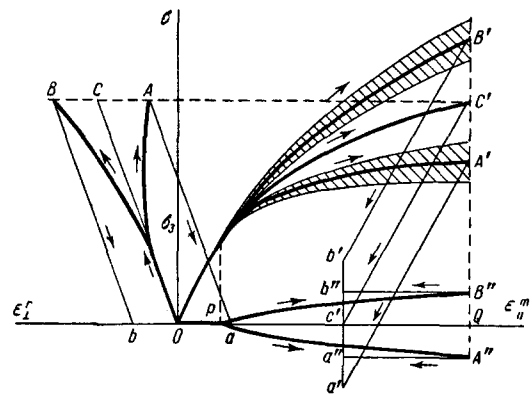


FIG. 5. Curve of deformation of a specimen consisting of weak A-domains and strong B-domains.⁹ OA and OB – x-ray deformation curves for weak A-domains and strong B-domains, OC – line corresponding to the condition $\sigma_r = \sigma_m$, OA' and OB' – curves of axial average structural stresses $\bar{\sigma}_{st}$ for A- and B-domains, OA'' and OB'' – curves of transverse average structural stresses $\bar{\sigma}_{2st}$, OC' – curve for σ_m . The shaded areas represent the zones of dispersion of structural stresses $\Delta\sigma_{st0}$. After macro-unloading there remain in the specimen average axial and transverse microstresses $\bar{\sigma}_{1i}$ and $\bar{\sigma}_{2i}$, represented respectively by the segments a'c', b'c', a''c'', and b''c'', and determined from the residual displacement of the x-ray lines by formula (1.8). The dispersion of the microstresses $\Delta\sigma_i$ is equal to the dispersion of the structural stresses $\Delta\sigma_{st}$ and is determined from the x-ray line broadening component β_s by means of formulas (3.1) and (3.41).

the mechanism proposed by Smith and Wood⁶⁰ were called by Rovinskii "oriented" microstresses. He assumes that the "oriented" microstresses first increase with increasing degree of plastic deformation and that their growth then slows down, since they gradually are converted into the usual "disoriented" microstresses.

Hauk⁸³ in an analysis of the dependence of $\Delta d/d$ on the angle between the normal to the (hkl) plane and the normal to the lateral surface of the specimen, concluded that the experimental results for metals containing "rigid" phases are explained by the third hypothesis, the only difference being that the "strong" domains are not the near-boundary domains, but the "rigid" phases. Vasil'ev and Erashev⁸⁴ also believed the third hypothesis to be correct. They concluded that after simple tension there is produced in the specimen a field of microstresses with components $\bar{\sigma}_{1i}$ and $\bar{\sigma}_{2i} = \bar{\sigma}_{3i}$. Vasil'ev⁸⁷ reached the same conclusion in an analysis of the changes in the dimensions of plastically-deformed specimens during the process of heating. Vacher et al.^{88,89} considered the third hypothesis to be correct. They also observed the presence of the components σ_{1i} , σ_{2i} , and σ_{3i} . In addition, it was found that transverse compressive stresses, amounting to 13 percent of the axial macrostresses,⁸⁹ arise in a stretched specimen when the yield point is passed.

Vasil'ev^{91,92} used angle photographs of small plane specimens cut out from plastically deformed larger specimens. He used formulas analogous to (1.8) to

calculate the microstresses. It was found that the microstress perpendicular to the surface exerts a noticeable influence on the position of the x-ray line. An analysis of the possible relations between the "oriented" microstresses $\bar{\sigma}_i$, determined from the shift of the x-ray lines, and the "disoriented" microstresses, determined from the broadening of the lines, has shown that the corresponding line broadening component β_s (see below) is due to oscillations (dispersion, $\Delta\sigma_i$) of the "oriented" stresses about a certain average value $\bar{\sigma}_i$, which is not equal to zero. The author believes that the terms "oriented" and "disoriented" microstresses are meaningless, and that the total microstress is equal to the sum of the average microstress $\bar{\sigma}_i$ and the dispersion $\Delta\sigma_i$

$$\sigma_i = \bar{\sigma}_i \pm \Delta\sigma_i. \quad (2.2)$$

The author assumes that in plastic deformations the A and B regions of the specimen are acted upon by "structural" stresses $\sigma_{st} \neq \sigma_m$ (Fig. 5), and that after the external load is removed this leads to the appearance of residual microstresses σ_i . The connection between σ_m , σ_{st} , σ_i , and $\Delta\sigma_i$, and the dispersion of the "structural" stresses $\Delta\sigma_{st}$ is given by the relations

$$\sigma_{st} = \bar{\sigma}_{st} \pm \Delta\sigma_{st} = \sigma_m + \bar{\sigma}_i \pm \Delta\sigma_i \quad (2.3)$$

and

$$\Delta\sigma_{st} = \Delta\sigma_i. \quad (2.4)$$

Experiments with previously stretched and compressed specimens of copper, nickel, aluminum, iron, and molybdenum have shown that the residual microstress acting on the matrix region is, after stretching,

$$\bar{\sigma}_{1i}^A < \bar{\sigma}_{2i}^A < 0, \quad (2.5)$$

and after compression

$$\bar{\sigma}_{2i}^A < \bar{\sigma}_{1i}^A < 0. \quad (2.6)$$

The "strong" B-domains (near-boundary regions) are acted upon, both after tension and after compression, by tensile microstresses, which exceed σ_m considerably, so that the "structural" stresses $\bar{\sigma}_{st}^B$ acting on the B-domain during plastic deformation will be tensile stresses in both cases. This is confirmed in references 92 and 93, in which $\bar{\sigma}_i$ and $\bar{\sigma}_{st}$ have been determined for cementite in high-carbon steel.

Macherauch and his co-workers⁹⁴⁻⁹⁸ obtained for aluminum, aluminum alloy, and copper the same angular dependences of $\Delta d/d$ as obtained in references 83, 91, and 92. While these later investigations have confirmed the third hypothesis, and the notion of the decisive role of the surface layer was refuted by etching or by cutting out small specimens,^{84,91} the hypothesis of the weakened layer was again advanced in references 97 and 98, although no test of its correctness (by removal of the outer layers of the specimen) was made.

The notion of the "oriented" microstresses^{60,86,91,92} was used also to analyze the following: the change in the dimensions of plastically-deformed specimens by heating,⁸⁷ the relaxation of aluminum and copper specimens,⁹⁹ the Bauschinger effect,^{100,101} a procedure for a separate determination of the macro- and microstresses,¹⁹ the deformation curve of soft steel,⁹⁸ the mechanism of deformation of large-crystal specimens,¹⁰² and the role of microstresses in the hardening of metals.¹⁰³

An analysis of the investigations reviewed in the present section leads to the following conclusions. The hypothesis of "weakened" layer⁴⁷ does not explain all the observed phenomena. In many cases there is either no weakened layer or its influence is negligibly small.⁷⁴ Experiments^{84,91} in which small samples have been cut out show that changes in the interplanar distances produce a volume effect. The observed "surface" effects are apparently due to technological factors.^{71,74} The Greenough hypothesis⁶² yields values of $\Delta d/d$ which are one order of magnitude smaller than those observed; in the best case this effect is superimposed⁸³ on the principal dependence which is well explained by the Wood hypothesis.⁶⁰ Since the values of $\Delta d/d$ (after Greenough) hardly exceed the experimental errors, it is impossible to decide at the present time whether the effect described by it exists. The hypothesis of weak regions in the matrix and strong near-boundary regions⁶⁰ explains the observed phenomena satisfactorily.

3. INVESTIGATION OF THE BROADENING OF X-RAY LINES

3.1. Possible Causes of Smearing of the Lines

Macroelastic deformation of a polycrystalline specimen should cause an insignificant reversible broadening of x-ray lines, if the elastic properties of the individual crystallites, which make up the specimen, are anisotropic. This circumstance was pointed out by Aksenov¹⁰⁴ and experimentally confirmed by Lihl,¹¹³ Schaal,¹⁰⁵ Aksenov and Moshchanskii,¹⁰⁶ and Brasse and Moller.¹⁰⁷

X-ray lines are broadened much more by plastic deformation. In the early work on this subject, the effect of broadening was wholly attributed to the development of microdistortions in the structure, characterized by changes in the interplanar spacing $\Delta d/d$, and to the occurrence of microstresses (residual stresses of the second kind¹⁰⁷⁻¹¹¹), corresponding to these microdistortions.¹⁰⁹⁻¹¹⁹ The relative change in the interplanar distances $\Delta d/d$ was determined from the formula

$$\beta_s = 4 \frac{\Delta d}{d} \operatorname{tg} \vartheta, \quad (3.1) *$$

* $\operatorname{tg} = \tan$.

where β_g is the line broadening due to the plastic deformation.

The corresponding microstresses σ_i were calculated either from the Secito formula,¹¹⁴ derived under the assumption of a linear stressed state:

$$\sigma_i = E \frac{\Delta d}{d}, \quad (3.2)$$

or from the Cagliotti-Sachs formula,¹¹¹ obtained for the case of all-sided tension (compression):

$$\sigma_i = \frac{3}{\chi} \frac{\Delta d}{d} = \frac{E}{1-2\mu} \frac{\Delta d}{d}, \quad (3.3)$$

where χ is the compressibility.

On the other hand, Selyakov¹²⁰ and Scherrer¹²¹ have shown that if the dimension of the particle (regions of coherent scattering) in a direction perpendicular to the reflecting plane is D , then the width of the x-ray line is determined by the formula

$$\beta_p = \frac{\lambda}{D \cos \vartheta}. \quad (3.4)$$

In contradiction to the microstress hypothesis, Wood¹²⁵⁻¹²⁷ has proposed that the line broadening in plastic deformation is due only to the fragmentation of the regions of coherent scattering (blocks), and that to each form of plastic treatment corresponds a minimum block dimension; when this is reached an increase in plastic deformation causes no further fragmentation, since recrystallization takes place already during the process of plastic deformation.¹²⁶

A criterion of the degree of smearing of the line in these investigations was the presence of a linear dependence of β on $\tan \vartheta$ [Eq. (3.1)] or on $\lambda \sec \vartheta$ [Eq. (3.4)]. Thus, Smith and Stickley¹²⁸ have established that for tungsten β depends linearly on $\tan \vartheta$, whereas the dependence of β on $\lambda \sec \vartheta$ gives a negative value of D as $\lambda \sec \vartheta \rightarrow 0$. In contrast to this, a

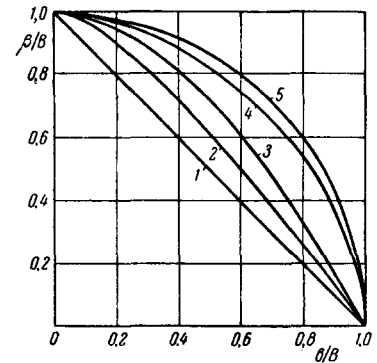


FIG. 6. Curves for correcting the widths of x-ray lines for instrument broadening. The curve marking is explained in Table I.

dependence of β on λ in accordance with Eq. (3.4) was observed in references 125 and 127. This method of analyzing the causes of broadening of the x-ray lines was criticized by Williamson and Hall,¹²⁹ who have shown that linearity of β with $\tan \vartheta$ or $\lambda \sec \vartheta$ cannot serve in practice as a criterion for the nature of the line broadening.

3.2. Correction for Geometrical Conditions of the Photography

An important source of reliable information on the causes of the broadening of x-ray lines is the method of finding the "physical" width, i.e., the method of eliminating from the total broadening the part due to instrumental causes.

At present the most widely used correction procedure is that proposed by Johnson.¹³⁰ He showed that if the intensity distribution in the experimental curve is described by the function $h(x)$, the integrated width of this line is B , and the corresponding functions and integrated widths for the "instrumental" curve and for the "physical" curve, due only to the imperfections in the crystal, are $g(x)$, b and $f(x)$, β respectively, then, apart from a constant factor,

Table I. Connection between B , b , and β for various cases

Authors	Form of functions $g(x)$, $f(x)$, and $h(x)$	Connection between B , b , and β	Curve on Fig. 6
Sherrer		$B = b + \beta$	1
Wood and Rachinger ¹²⁷	$(1 + k^2 x^2)^{-1}$	$B = b + \beta$	1
Warren and Biscoe ¹²²	$\exp(-k^2 x^2)$	$B^2 = b^2 + \beta^2$	5
Jones ¹³⁰	a) $g(x) = (1 + x^2)^{-2}$, $f(x) = (1 + k^2 x^2)^{-1}$; $g(x)$ determined from experiments	$\frac{\beta}{B} = 2\rho$, $\frac{b}{B} = k\rho$, $\rho = \frac{2k^3 - k^2 + 1}{2(1 - k^2)}$	2
	b) $f(x) = (1 + k^2 x^2)^{-1}$, c) $f(x) = \exp(-k^2 x^2)$	curves $\frac{\beta}{B} = f\left(\frac{b}{B}\right)$	4
Taylor ¹²³		$\beta^2 = (B - b)(B^2 - b^2)^{\frac{1}{2}}$	—
Schoening, Niekerk, and Haul ¹²⁴	$g(x) = \frac{C_1}{(1 + k_1 x^2)^2}$, $h(x) = \frac{C_2}{(1 + k_2 x^2)^2}$	curve $\frac{\beta}{B} = f\left(\frac{b}{B}\right)$	3
Lysak ¹³³	$g(x) = (1 + k_1 x^2)^{-2}$, $f(x) = (1 + k_2 x^2)^{-1}$	curve $\frac{\beta}{B} = f\left(\frac{b}{B}\right)$	2

$$h(x) = \int_{-\infty}^{\infty} f(y) g(x-y) dy \quad (3.5)$$

and

$$B = \frac{b\beta}{\int_{-\infty}^{\infty} f(x) g(x) dx} \quad (3.6)$$

The standard, i.e., the specimen from which the g curve is obtained, is usually an annealed specimen made of the investigated material.

Thus, to determine the value of β it is necessary to know the form of $f(x)$ and $g(x)$. The simplest but not always sufficiently reliable method of finding β from known B and b with the aid of relations (3.6) is to pick analytic functions for $f(x)$ and $g(x)$. The connection between B , b , and β for different functions $h(x)$, $g(x)$, and $f(x)$, chosen by various authors, is listed in Table I, and it is sometimes more convenient to determine this connection graphically from the relation $\beta/B = f(b/B)$, plotted in Fig. 6. It must be borne in mind that one must substitute in (3.6) the values obtained for B and b already after separating the K doublets by one of the known methods.^{30-32,130,131}

A shortcoming of the Jones comparison method¹³⁰ is that it is impossible to pick accurately analytic functions that describe the real profile of the x-ray line. The choice of various functions can change the results appreciably, and to a greater extent for the forward lines (i.e., large b/B). For example, when $b/B = 0.8$ the values of β/B for curves 1 and 5 (Fig. 6) differ by a factor of three, but for $b/B = 0.2$ the difference is on the order of 20 percent. An analysis of the errors due to the use of the Jones method is given in references 132 and 133.

Kochendorfer¹³² (see also reference 134) developed an absolute method of accounting for instrumental errors, in which allowance is made for the size of the collimator diaphragm, the photometer slit, the $K\alpha$ doublet, the "natural width" of the spectral lines, the dimension and shape of the specimen, and the absorption in the specimen. An absolute method of accounting for instrumental errors was also proposed by Bértaut.¹³⁵

The accuracy of finding the f -curve can be appreciably increased by harmonic analysis. From the theory of Fourier transformations it is known¹³⁶ that if $F(t)$ and $G(t)$ are the transforms of the functions $f(x)$ and $g(x)$, i.e., the coefficients of the Fourier series

$$\left. \begin{aligned} f(x) &= \sum_{-\infty}^{\infty} F(t) \exp\left(-2\pi i t \frac{x}{a}\right), \\ g(x) &= \sum_{-\infty}^{\infty} G(t) \exp\left(-2\pi i t \frac{x}{a}\right), \end{aligned} \right\} \quad (3.7)$$

where $\{(-\alpha/2, \alpha/2)\}$ is the expansion interval, then the transform $H(t)$ of the function $h(x)$ is $F(t)G(t)$, i.e.,

$$H(t) = F(t)G(t). \quad (3.8)$$

To find the coefficients $H(t)$ and $G(t)$, Schull¹³⁷ approximated the profiles of the x-ray lines by means of the function

$$g(x) = \exp(-m^2x^2), \quad (3.9)$$

$$h(x) = \exp(-p^2x^2) + \tau \exp(-q^2x^2) \quad (3.10)$$

and calculated analytically the coefficients $F(t)$. This method, however, has the same shortcoming, the need of picking the analytic functions.

Stokes¹³⁸ proposed a numerical method, free of these shortcomings, wherein the coefficients $H(t)$ and $G(t)$, and consequently also $F(t)$, are determined from the experimental h and g curves with the aid of the Lipson-Bever strips. In the Soviet literature, this method was described in detail in the book by Pines.¹³⁹

3.3. Separate Determination of the Broadening Effects

Relations (3.5) and (3.6) can also be readily used for a separate determination of the smearing effects caused by microstresses and fragmentation of the blocks. Actually, if we denote by $s(x)$ and $p(x)$ the functions that describe the distribution of the intensity in the components of the f curve, due respectively to the influence of microstresses and block fragmentation and the corresponding integral widths by β_s and β_p , then

$$f(x) = \int_{-\infty}^{\infty} s(y) p(x-y) dy \quad (3.11)$$

and

$$\beta = \frac{\beta_s \beta_p}{\int_{-\infty}^{\infty} s(y) p(y) dy} \quad (3.12)$$

In order to find in explicit form the connection between β , β_s , and β_p from Eq. (3.12), it is necessary to specify the form of the s and p functions. However, compared with the solution of the analogous problem of finding the connection between B , b , and β , additional difficulties arise here, connected with the fact that it is usually impossible to obtain "pure" s and p curves in an investigation of plastic deformation, since the fragmentation of the regions of coherent scattering is accompanied by the development of microstresses. At the same time, by specifying the form of the s and p functions in some manner, we predetermine to a certain degree the result of the separation.

Lysak¹⁴⁰ recommends that the s and p functions be found for specially prepared specimens, which give "pure" effects of one kind only, under the assumption that the form of the s - and p -curves will not change in a specimen where both causes of broadening are simultaneously active.

Kochendorfer^{132,134} used instead of the integral width the half-width of the line, $b_{1/2}$, and picked the s function in the form of a rectangle and the p function in the form of a triangle, obtaining the relation

$$\text{and } \left. \begin{aligned} b_{1/2} &= \frac{b_p}{1 - \frac{b_s}{4b_p}} \quad \text{for } b_s < 2b_p \\ b_{1/2} &= b_s \quad \text{for } b_s \geq 2b_p. \end{aligned} \right\} \quad (3.13)$$

Kurdyumov and Lysak¹⁴¹ have assumed that the s and p curves are described by Gauss' functions; then

$$\beta^2 = \beta_s^2 + \beta_p^2. \quad (3.14)$$

Hall¹⁸³ took these functions in the form $(1 + k^2 x^2)^{-1}$, which leads to the relation

$$\beta = \beta_s + \beta_p. \quad (3.15)$$

Lysak¹⁴⁰ took the s function in the form $(1 + k_1^2 x^2)^{-2}$, and the p function in the form $(1 + k_2^2 x^2)^{-1}$, as a result of which he obtained

$$\beta = \frac{(\beta_p + 2\beta_s)^2}{\beta_p + 4\beta_s}. \quad (3.16)$$

To find $\Delta d/d$ and D , it is necessary to have at least two x-ray lines and to use two orders of reflection from one plane, owing to the possible anisotropy of $\Delta d/d$ and D .

We note in addition that when the block and microstress effects are so separated, an important role is played not only by the choice of the s and p functions, but also by the method of separating the geometrical factor. The point is that the cause of the broadening and the share of each of the effects are determined by the ratio of broadening of two lines, β_2/β_1 , and in the general case we have

$$\frac{\sec \vartheta_2}{\sec \vartheta_1} \leq \frac{\beta_2}{\beta_1} \leq \frac{\operatorname{tg} \vartheta_2}{\operatorname{tg} \vartheta_1}. \quad (3.17)$$

But the value of β_2/β_1 will vary greatly with the method chosen to determine β , since the transition from one of these to the other manifests itself essentially in small-angle deflections, i.e., in β_1 (Fig. 6). Thus, by specifying a definite form of the functions $g(x)$ and $f(x)$, an evaluation of β predetermines to a certain degree the resultant values of β_s and β_p .

In the case of isotropic blocks this method of separating the effects presupposes that D is independent of the indices of the reflecting plane. As shown recently by Khachatryan,¹⁶⁷ however, this is not at all so. He considered the connection between the size of the mosaic block, L_{b1} and that of the region of coherent scattering, D . It was found that $D = L_{b1}$ only when $L_{b1}\bar{\alpha} \gg d$, where $\bar{\alpha}$ is the average disorientation of the blocks. In all the remaining cases $D > L_{b1}$, owing to the presence of a coherent bond between the neighboring blocks. When $L_{b1}\bar{\alpha} > d$ we have

$$D \approx L_{b1} + \frac{d}{\sqrt{2\pi\bar{\alpha}}}. \quad (3.18)$$

This circumstance causes the dimension of the region of coherent scattering to depend on the indices of diffraction, and the angular dependence of the component β_p is intermediate between $\sec \vartheta$ and $\tan \vartheta$. As a result, relations (3.1) and (3.4) do not separate unambiguously the spreading due to microdistortions from that due to block fragmentation.

3.4. Separation of the Effects by Harmonic Analysis of the Line Shape

Warren and Averbach¹⁴²⁻¹⁴⁷ proposed an analysis method based on the study of the forms of the f lines themselves, not merely their integrated widths (in the Soviet literature this method is detailed in references 139 and 148). They have shown that the distribution of the intensity of the f lines can be expressed as

$$f(2\vartheta) = K \sum_n A_n(l) \cos 2\pi h_3 n + B_n(l) \sin 2\pi h_3 n, \quad (3.19)$$

where $h_3 = (2a_3/\lambda) \sin \vartheta$ is the running coordinate in reciprocal space; A_n and B_n are the coefficients of the expansion of $f(2\vartheta)$ in the interval $-\frac{1}{2} < \Delta l < \frac{1}{2}$; N is the total number of cells (in the volume of the specimen exposed to the x-rays); l is the index of the reflecting plane in the $(00l)$ reciprocal lattice system, chosen such that l coincides with the normal to the reflecting plane; a_3 is the period along the normal to the reflecting plane with $l = a_3 l_0 / a = (a_3/a) \sqrt{\sum h_i^2}$, where h_i are the usual indices of the reflecting plane. The coefficients A_n and B_n are determined in practice by a method described previously.¹³⁸

For most metals and even for nonmetals¹⁴⁹ the line broadening after plastic deformation is symmetrical. Therefore, since the analysis thus far did not take into account the aforementioned line shift, and the new position of the line peak was simply taken as a new reference point, the coefficients B_n were assumed to be equal to zero. We denote by A_n^S the Fourier coefficients of the function $q(ne_n)$, describing the distribution of the microstresses (relative deformation) e_n in the structure, and by A_n^P the Fourier coefficients of the function $f(j)$, which describes the distribution of the particles by dimensions, where j is the number of cells in a "column"; then, according to Eqs. (3.8) and (3.11)

$$A_n = A_n^S A_n^P, \quad (3.20)$$

with

$$A_n^S = \overline{\cos(2\pi l Z_n)}, \quad (3.21)$$

$$A_n^P = \frac{1}{N} \int_{j=n}^{\infty} (j-n+1) p(j) dj. \quad (3.22)$$

Here and henceforth the superior bar denotes averaging, and Z_n is the displacement component expressed in fraction of the lattice axis along the normal to the reflecting plane, with

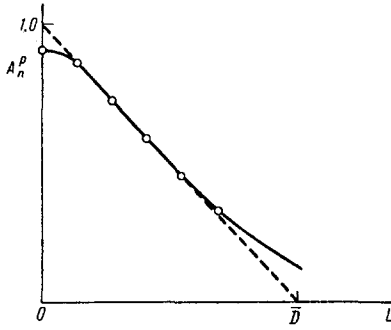


FIG. 7. Dependence of the coefficients A_n^P on the distance L . Methods are indicated for determining \bar{D} and finding the coefficient A_n^P in the presence of a "hook" in the curve $A_n^P=f(L)$.^{3,166}

$$Z_n = ne_n. \quad (3.23)$$

The function $q(ne_n)$ is determined from the relation

$$q(ne_n) = \int_0^{\infty} A_n^S \cos(2\pi l_0 Z_n) dl_0. \quad (3.24)$$

Averbach and Warren have shown that if Z_n is small or if $q(ne_n)$ is described by a Gaussian function

$$q(ne_n) \sim \exp - \frac{e_n^2}{2e_n^2}, \quad (3.25)$$

then

$$A_n^S = \exp(-2\pi^2 l^2 n^2 \bar{e}_n^2). \quad (3.26)$$

Williamson and Smallman¹⁵⁹ assume that

$$q(ne_n) \sim \left(1 + \frac{e_n^2}{\bar{e}_n^2}\right)^{-1}, \quad (3.27)$$

which yields

$$A_n^S = \exp(-2\pi l n \bar{e}_n), \quad (3.28)$$

where \bar{e}_n is the half-width of the Cauchy distribution function (3.27).

Kochendorfer and Wolfstieg¹⁵⁰ have shown that for sufficiently small n , any "bell-shaped" distribution can be replaced with accuracy sufficient for practical purposes by a Gaussian curve (3.25).

Even before that, Bertaut has shown¹⁵¹ that

$$\left. \frac{dA_n^P}{dn} \right|_{n=0} = -\frac{1}{\bar{N}_3} \quad (3.29)$$

and

$$\frac{d^2 A_n^P}{dn^2} = \frac{p(n)}{N}, \quad (3.30)$$

where \bar{N}_3 is the average number of cells in the column.

Thus, by drawing a tangent to the A_n^P vs n curve at the point $n = 0$, we can find \bar{N}_3 , and hence the average dimension of the "column" (block) $\bar{D} = \bar{N}_3 a_3$ in the direction perpendicular to the reflecting plane. If we plot the dependence of A_n^P on the distance in the lattice $L = na_3$, then the intercept of the tangent on the abscissa axis will be equal to \bar{D} (Fig. 7).

A separate determination of A_n^S and A_n^P is carried out with the aid of relation (3.20), with allowance for

the fact that A_n^P should be independent of l , so that the dependence of A_n on l at $l = 0$ yields the value of A_n^P . Since, according to (3.20),

$$\ln A_n = \ln A_n^S + \ln A_n^P, \quad (3.31)$$

the dependence of $\ln A_n$ on l^2 should be linear in the case of the distribution given by (3.25); if the distribution (3.27) is used, a straight line is obtained as a function of l . Obviously, we can determine A_n^S and A_n^P without knowing the function $q(ne_n)$ only if there are at least three orders of reflections; if the form of the function $q(ne_n)$ is known, it is enough to have two orders of reflection from the (hkl) plane.

Brasse and Moller,¹⁵² using molybdenum $K\alpha$ radiation and a scintillation counter, found for steel after 5% plastic deformation and for small values of n that the function $q(ne_n)$ has a Cauchy distribution; an increase in n leads to a Gaussian distribution. After deformation to 20%, the distribution function is close to Gaussian. Schoening and Niekerk,^{153,154} using powdered silver and solid silver specimens, also found that $q(ne_n)$ fits a Gaussian curve. This function is picked in most present day investigations.

Pines¹⁵⁵ described a method of determining A_n^S and \bar{D} with the aid of only one order of reflection from the (hkl) plane. Since

$$\left. \frac{dA_n}{dn} \right|_{n=0} = \left. \frac{dA_n^P}{dn} \right|_{n=0}, \quad (3.32)$$

the tangent to the curve A_n at the point $n = 0$ yields the average dimension \bar{D} of the "columns." Further, neglecting the size distribution of the particles, it is also possible to determine with the aid of (3.20) the coefficients A_n^S . Another method indicated by Pines consists of approximating $q(ne_n)$ and $p(j)$ by means of analytic functions.

Garrod and Auld⁴⁴ also used one reflection to separate the spreading effect. It was found that for small n the dependence

$$-\frac{\ln A_n}{n} = f(n) \quad (3.33)$$

is a straight line whose slope and intercept with the ordinate axis determine \bar{e}_n^2 and \bar{N}_3 .

Hauk and Hummel⁴⁵ indicated the possibility of determining \bar{e}_n^2 from a plot of

$$\frac{1-A_n}{n} = f(n), \quad (3.34)$$

drawn for only one order of reflection. An analogous method was described by Shvirin.¹⁵⁶

Of great importance to an estimate of the singularities in the Warren-Averbach method are the works of Eastbrook and Wilson,¹⁵⁶ Garrod, Brett, and Macdonald,¹⁵⁸ and Williamson and Smallman.¹⁵⁹ It was shown in these investigations that an inaccurate measurement of the ordinates of the profile of the x-ray line near the background line, i.e., precisely where the measurement errors increase, affects greatly the magnitude of

Table II

Material	State	After Kochendorfer ¹³²		s(x) and p(x) - Cauchy function ¹⁸³		s(x) and p(x) - Gaussian functions ¹⁴¹		Harmonic analysis		Reference
		$D \cdot 10^8$, cm	$\frac{\Delta d}{d} \cdot 10^3$	$D \cdot 10^8$, cm	$\frac{\Delta d}{d} \cdot 10^3$	$D \cdot 10^8$, cm	$\frac{\Delta d}{d} \cdot 10^3$	$\bar{D} \cdot 10^6$, cm	$\sqrt{e_n^2} \cdot 10^3$	
Silicon steel 55 C ₂	Compression by 66.3%, filed powder	—	—	20	2.28	3.3	2.35	2.8	2.1	162
35 KhNM steel	Tension to rupture	3.5	0.67	∞	4.65	2.8	5.0	2.8	4.6	160
Hadfield steel	Compression 30%	—	—	6.0	0.7	—	—	4.0 *	1.5 *	161
Steel 45	Compression 50% plus heating at 450° C (10 minutes)	—	—	—	—	6.0	1.0	6.1 *	1.95 *	163
Carbon steel with 0.24% C	Tension 4%	>2	1.64	16	0.96	—	—	200 *	2.5 *	45
Gray cast iron	0.11	15	0.2	15	0.12	—	—	700	1.8	45
Carbon steel with 0.16% C	Loading in macroelastic region	6.4	0.57	—	—	4.7	0.57	4.0	0.71	107
Tungsten	Unloaded	9.8	0.16	—	—	5.9	0.72	2.7	0.41	107
Silver	Powder	—	—	4.9	0.8	—	—	2.4	2.5	154
				3.3	1.3	—	—	1.8	1.5	
Nickel	Powder			23				5 (10) **	7 (12)	254
Iron	Powder							0.3 (1,0)	3 (8)	159
Molybdenum	Powder							0.5 (∞)	4 (8)	169

*With one order of reflection.

**The numbers in the parentheses are for a Cauchy distribution of the microstresses, in all other cases - for a Gaussian distribution.

the Fourier coefficients when n is small, and consequently, may lead to large errors in the determination of D and $\sqrt{e_n^2}$. Apparently, this pertains in particular to curves obtained by the photomethod, where the background line may not be drawn sufficiently accurately, and the usual tendency is to exaggerate the background line.

Hauk and Hummel,⁴⁵ using specimens of cast iron and steel and a powder of colloidal silver, determined D and $\sqrt{e_n^2}$ by the methods of Kochendorfer,¹³² Haul,¹⁸³ and Averbach-Warren. For all specimens, the last method gave values of \bar{D} and $\sqrt{e_n^2}$ one order of magnitude greater than the first two methods and the values of \bar{D} as determined by an objective method for a specimen made of colloidal silver. The authors attribute this result to the extreme sensitivity of the Warren-Averbach method to the position of the background line, and assume that the determination of D and $\sqrt{e_n^2}$ with the aid of the integral width should be given preference over the Averbach-Warren method.

Along with this, it was observed in many investigations that the values of D and $\sqrt{e_n^2}$ determined by methods using the integral width agree well with those obtained by the Warren-Averbach method (see Table II).

Kochendorfer and Walfstiegl¹⁵⁰ have shown that the use of at least two orders of reflection increases appreciably the reliability of determination of \bar{D} and $\sqrt{e_n^2}$ in comparison with methods in which only one order is used.

Of great importance to the estimate of methods used for the determination of \bar{D} and $\sqrt{e_n^2}$ with only one order of reflection is the analysis of the "hook" effect, described by Warren and his co-workers.^{165,166} The A_n^D vs n curve should not have a negative second derivative, for according to (3.30) this has no physical meaning. Actually, however, real curves do exhibit an inadmissible bending of the curve in the region of small n (see Fig. 7). This is explained^{3,166} by the almost unavoidable exaggeration of the background line in plotting the profile of the x-ray curve. To exclude these systematic errors it is proposed to determine the values of A_n^D by extrapolating the linear portion of the curve A_n^D until it intersects the ordinate axis, with a suitable recalculation of the remaining coefficients.

In addition, Bertaut¹³⁵ has shown even earlier that an analogous deviation from linearity of the initial portion of the A_n^D curve may be caused by the "finite summation," i.e., by the limitation of the summation interval. If correctly chosen, the latter should overlap the width of the line by at least a factor of 3.

The foregoing effects may distort excessively the results of the determination of \bar{D} and $\sqrt{e_n^2}$ with only one order of reflection. Thus, Smirnov,¹⁶⁸ using the Pines method,¹⁵⁵ has noted that no sharply pronounced tangent to the A_n curve is observed, and the experimentally determined values of \bar{D} may differ by one order of magnitude as the expansion interval is increased by 12.5 times. Wagner¹⁶⁹ states that methods involving a single line cannot be used at all.

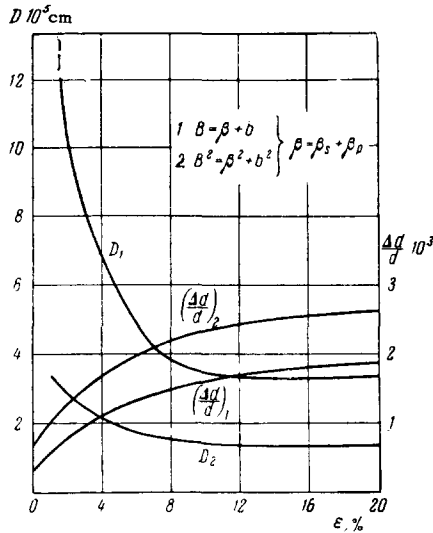


FIG. 8. Dependence of D and $\Delta d/d$ on the degree of deformation of steel No. 15.¹⁷³

3.5. Change in Size of Blocks and Microdistortions in Deformation of Metals

It is now established by numerous investigations^{129, 146, 156, 159, 163, 170, 177, 179, 180-185, 188} that plastic deformation of metals produces in the specimens both microstresses and fragmentation of the regions of coherent scattering. Both effects increase noticeably with increasing plastic deformation, but only up to a certain limit, after which their growth slows down.

Rovinskii^{172, 173} proposes that no further crumbling occurs at high degrees of plastic deformation, because of the "capture" effect, i.e., the growth of excessively small blocks even during the deformation process. Figure 8 shows the changes in the blocks and microdistortions, obtained by Rovinskii for steel. The effects are seen to vary with the methods used to determine β . There are reports¹⁷⁵⁻¹⁷⁷ of a second increase in $\Delta d/d$, accompanied by an increase in the hardness H , after large degrees of plastic deformation (on the order of 70 - 80 percent).

Usually a direct proportionality is observed^{176, 178, 179} between the microstresses $\Delta d/d$ and the hardness of the material H corresponding to the deformed state, and likewise between the microdistortions and the yield point in the deformed state.¹⁷⁹⁻¹⁸² It should be noted that the yield point in the deformed state practically coincides with the microscopic stress σ_m in the specimen prior to unloading. A similar linear dependence is observed^{52, 112, 113} between the over-all width of the line and the characteristics of the resistance to plastic deformation σ_m and H . In plastically deformed aluminum, copper, and nickel under normal and reduced temperatures, according to Paterson,¹⁸⁰ the dependence of the broadening of the line on the degree of plastic deformation has the same form as the strain curve. An analogous dependence was observed by

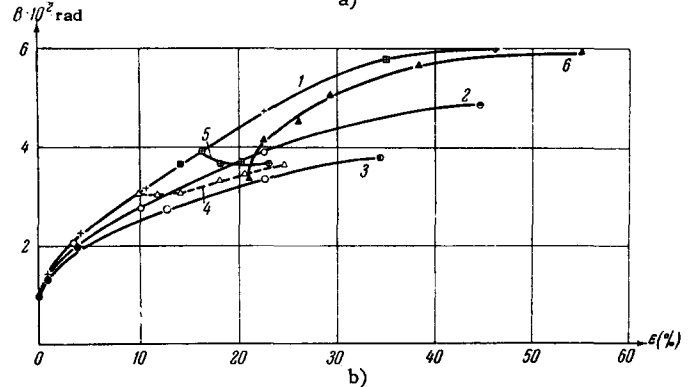
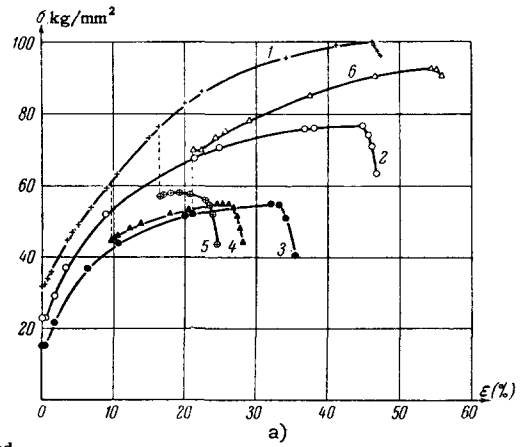


FIG. 9. Tension diagrams of nickel (a) and dependence of the width of the 420 x-ray line on the degree of deformation (b) at different temperatures.¹⁸⁵ 1 - 2°K; 2 - 77°K; 3 - 300°K; 4 and 5 - 300°K and after deformation at 4.2°K; 6 - 4.2°K and after deformation at 300°K.

Davidenkov and Smirnov¹⁸⁴ and by Klyavin and Smirnov¹⁸⁵ in nickel, molybdenum, iron, and tungsten (Fig. 9).

In earlier investigations it was concluded on the basis of these relationships that the microdistortions are greatly responsible for the hardening. It became necessary to forego this straight-forward point of view, for in many cases^{115, 116, 176, 178, 186} of tempering of plastically deformed specimens the microdistortions diminish almost to zero, whereas the hardness changes little, or even increases.

Kurdyumov and his co-workers^{176, 178, 186} propose that the microdistortions are not the direct cause of the high hardness and high resistance to deformation of the hardened metal, but are merely a characteristic of the limit of elastic deformation of the metal in microvolumes.

Vasil'ev^{91, 92} believes that the value of $\Delta d/d$, determined from the broadening component β_s by formula (3.1), is a measure of the difference between the "structural" stresses σ_{st} , acting on individual domains of the specimen, and the average "structural" stresses $\bar{\sigma}_{st}$ (see Fig. 5).

Rovinskii and Rybakova¹⁷² have found that the following relation holds true over a considerable range of strains

$$\frac{\Delta d}{d} D = \text{const} \rightarrow \Delta d. \quad (3.35)$$

That the product $\bar{D}\sqrt{e_n^2}$ is constant is noted also by Despujols and Warren.¹⁸⁷

Rovinskii and Rybakova¹⁸⁸ have observed in plastically deformed steel specimens a direct proportionality between the yield point in the deformed state and the quantities $(\Delta d/d)^{1/2} D^{-1/2}$, and also a linear dependence of the hardness H on the product $\left(\frac{\Delta d}{d} \frac{1}{D}\right)^{1/2}$.

This last dependence is noted also in reference 163.

Without discussing the fragmentation of the regions of coherent scattering and hardening of the metal in plastic deformation, considered in references 3, 161, 172, 173, 176, 177, 186, and 189–191, let us dwell on the possibility of going from the microdistortions $\Delta d/d$ to the corresponding microstresses. As already noted, the idea that a knowledge of the microdistortions will enable us to calculate the microstresses σ_i , has been predicted already in the early papers devoted to plastic deformation. The other extreme point of view denies in general the possibility of determining the stresses, in the sense of the theory of elasticity, from data on microdistortions.¹⁹¹ According to the dislocation theory¹⁹² the field of the microstresses is none other than the far field of the dislocations produced during plastic deformation.

Stokes and Wilson¹⁹³ have proposed that the microstresses σ_i are statistically and isotropically distributed in a polycrystalline specimen. If it is assumed that all values of microdeformations between zero and the maximum value e_{\max} are equally probable, then the integral width β_s will be

$$\beta_s = 4e_{\max} \operatorname{tg} \vartheta, \quad (3.36)$$

which coincides with the expression (3.1) with $e_{\max} = \Delta d/d$. In case of a Gaussian microdeformation distribution we have

$$\beta_s = 2(2\pi e^2)^{1/2} \operatorname{tg} \vartheta. \quad (3.37)$$

In the former case, averaging over all directions with allowance of only the normal components of the microstresses yielded the expression

$$\beta_s \operatorname{ctg} \vartheta = A + B\Gamma, \quad (3.38)^*$$

where A and B are functions of the microstresses and the elastic constants, and Γ is an orientation factor for the (hkl) planes. In the latter case both the normal and tangential components of the microstress tensor were taken into account in the averaging, and this yielded

$$\beta_s \operatorname{ctg} \vartheta = (A + B\Gamma)^{1/2}. \quad (3.39)$$

The authors have reached the conclusion that the low accuracy of the experimental data makes neither of the discussed versions preferable, although the Gaussian distribution appears to be the more probable.

Blachman¹⁹⁴ considered various types of relations between the microdeformations and the microstresses. For the simplest model of a statistically isotropic distribution of microstresses he obtained

$$e = (s_{11} + 2s_{12}) \sigma_i, \quad (3.40)$$

where s_{11} and s_{12} are known elastic constants; this agrees with (3.3). Blachman assumed that this simplest model should give good agreement with experiment in plastically deformed tungsten.

Vasil'ev⁹¹ proposes that the component β_s yields not the total microstress σ_i , but only its dispersion $\Delta\sigma_i$ (see above), with $\Delta\sigma_i$ defined as

$$\Delta\sigma_i = \frac{E}{1+2\mu} \frac{\Delta d}{d}, \quad (3.41)$$

where $\Delta d/d$ is determined from (3.1).

The hypothesis of statistically isotropic distribution of microstresses was verified by Smith and Stickley¹²⁸ in deformed α -brass and tungsten; by Stokes, Pascoe, and Lipson¹⁹⁵ in copper powder; by Megan and Stokes¹⁹⁶ in iron, nickel, copper, silver, aluminum, and lead powders; by Hall,¹⁸³ who used data obtained by many investigators; by Auld and Garrod^{43,44} in powders and solid deformed iron specimens; and by Warren and Averbach¹⁴⁵ in α -brass. In all cases, the product of the microdeformations by the corresponding modulus of elasticity remained constant, confirming the hypothesis of statistically isotropic distribution of σ_i .

Shivrin¹⁵⁶ obtained no confirmation of this hypothesis in experiments with medium carbon steel. It should be noted that Shivrin used the values of E_{hkl} calculated for a single crystal,¹⁹⁷ whereas in reference 44, for example, the elastic moduli were calculated by the Neerfeld method.⁴¹

Vasil'ev⁹¹ did not observe any dependence of the line broadening on the angle between the (hkl) plane and the strain axis in plastically deformed (by tension or compression) specimens of low-carbon steel; this is also in agreement with the hypothesis of isotropic distribution of the microstresses or of the microstress dispersion, in Vasil'ev's terminology.

Let us examine the quantitative connection between the microstresses calculated from the line broadening and the macroscopic characteristics of resistance to deformation. Cagliotti and Sachs¹¹² found that the microstresses in single-crystal and polycrystalline copper specimens amount to 0.25–0.33 of σ_m . Kurdyumov and co-workers¹⁷⁶ found that the microstresses in alloyed ferrite are 0.3 of the yield point in the deformed state and approximately equal to the yield point in the undeformed state. Sandler¹⁷⁹ observed that the microstresses in iron specimens are likewise equal to 0.3 of the yield point in the deformed state. A similar conclusion was reached by Khotkevich and his co-workers.¹⁸¹ Smith and Stickley¹²⁸ found that the microstresses in α -brass and in tungsten are equal to the ultimate resistance of the metal; a similar result was

*ctg = cot.

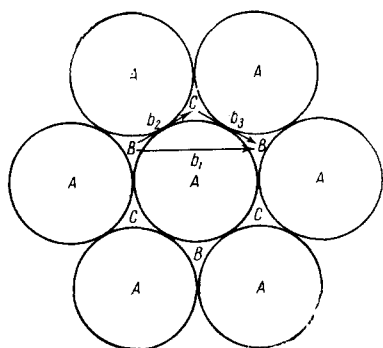


FIG. 10. Arrangements of atoms in the close-packing plane of the fcc lattice

$$\begin{aligned} \mathbf{b}_1 &= \frac{1}{2} a [10\bar{1}], \\ \mathbf{b}_2 &= \frac{1}{6} a [2\bar{1}\bar{1}], \\ \mathbf{b}_3 &= \frac{1}{6} a [11\bar{2}]. \end{aligned}$$

obtained by Megan and Stokes¹⁹⁶ for powders of iron, nickel, copper, silver, aluminum, and lead. It should be noted that the hypothesis that the microstresses are equal to the yield point in the deformed state was advanced already by van Arkel.¹⁰⁹ Except in reference 111, the microstresses were calculated from (3.2), using either the "macroscopic" modulus of elasticity E_m or the modulus E_{hkl} calculated for the single-crystal specimen.

The foregoing investigations were devoted essentially to a clarification of the physical nature of the effects that lead to the broadening of the x-ray lines. In addition, the procedures described were used in many investigations to study the microdistortions and crumbling of blocks due to fatigue,¹⁸⁸⁻²⁰² creep,^{160,203,204} irradiation,²⁰⁵⁻²⁰⁹ surface hardening,²¹⁰⁻²¹³ and cavitation.²¹⁴

4. EFFECT OF STACKING FAULTS ON THE DIFFRACTION OF X RAYS

It has been shown recently that the broadening and shift of x-ray lines can be due not only to factors mentioned above, but also to stacking faults in the crystal lattice. It was found that in various types of crystal lattices the stacking faults influence the change in the x-ray patterns differently. In the present paper we consider only structures with face-centered cubic and body-centered cubic lattices.*

4.1. Face Centered Cubic Lattice

There are two types of close-packed structures, face centered cubic (fcc) and hexagonal close-packed (hcp); the atoms in these structures have the closest packing. The arrangement of the atoms in close packing is shown in Fig. 10. If the atoms in one layer (layer A) are close-packed, then the atoms of the next layer can occupy either positions B or C. Both layer arrangements yield a close-packed structure. The fcc structure is obtained from the sequence ABCABC... (Fig. 11a) where the fourth layer is located above the first, whereas in the hcp structure the third layer is located

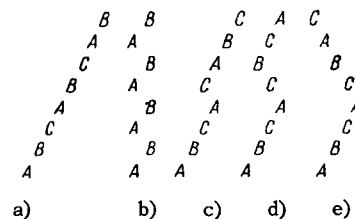


FIG. 11. Location of atoms in close-stacked planes. a) Normal fcc lattice; b) normal hcp lattice; c) intrinsic fault (single deformation fault); d) extrinsic fault (double deformation fault); e) growth or twin fault.

vertically above the first layer, the sequence ABABAB... is observed (Fig. 11b). The (111) planes are close packed in the fcc, and the base planes in the hcp.

Deviations from the normal alternation of the atomic planes are faults in their stacking order.* In an fcc lattice any sequence of three (111) atomic planes, which does not have the order ABC or CBA, is faulty. Examples of possible stacking faults are shown in Fig. 11. If the layer B, which follows the layer A, is placed in position C, we have a new defective sequence ABCACABC..., which contains four layers of the hcp lattice (Fig. 11c). Such a fault is called^{216,217} a fault of the subtraction type (intrinsic fault); it is formed by subtracting one layer (in this case B) from the regular sequence. If each succeeding layer following the first fault is shifted in accordance with the same law, we obtain the sequence ABC(A)CBA..., which represents a twin in the fcc structure (Fig. 11e). The two sequences ABC and CBA describe the fcc structure equally well, i.e., there is only one disturbance CAC here, which is called a growth fault or a twin fault (coherent twin boundary). The smallest possible twin contains two layers. The letter symbol for it is ABCACBCA, where the layers BCACB form a twin. A defect of this kind is called an intrusion fault (extrinsic fault); it is formed if an additional plane is added to the regular sequence (in this case C). Intrinsic and extrinsic faults have two twin boundaries each. Inasmuch as they are obtained as the result of plastic deformations, they are frequently called deformation faults.

Barrett²¹⁸ first called attention to the fact that plastic deformation in some metals and alloys is accompanied by stacking faults which may cause broadening of the x-ray lines. Starting from qualitative results on the change of the broadening ratio β_{200}/β_{111} after deformation, he concluded that the broadening due to stacking faults cannot be neglected.

Paterson²¹⁹ determined quantitatively the influence of intrinsic stacking faults on the width and position of x-ray lines under the assumption that each crystal contains faults only in one row of parallel lines, and that

*The effect of stacking faults in the case of hexagonal close-packed lattices (h.c.p.) are discussed in references 4 and 215.

*Faults in the stacking of the close-packed planes will henceforth be called simply faults.



FIG. 12. Effect of deformation faults on the x-ray diffraction pattern.²¹⁹

each fault extends over the entire crystal. He found that influence of the stacking fault depends on the indices of the reflecting planes, and that if $h + k + l = 3N$, where N is an integer, then the reflection neither spreads nor shifts; on the other hand, if $h + k + l = 3N \pm 1$, a broadened reflection is obtained, shifted towards the larger or smaller angles, respectively. For examples, the planes (111) and $(\bar{1}\bar{1}\bar{1})$ yield unbroadened and unshifted components, while the remaining {111} planes give broadened lines shifted towards the larger angles. By examining in this manner all the (hkl) families, we can obtain a complete picture of the influence of the stacking fault. This is shown schematically in Fig. 12, where the vertical lines show the sharp components, while the shaded areas are the broadened components. The arrows indicate the direction of the shift, and the figures give the number of components.

If we denote the probability of finding a stacking fault in any given layer by α (i.e., there is one fault every α^{-1} planes), we obtain the following quantitative relations:²¹⁹

1) broadening β of an individual component is symmetrical, with

$$\beta = 3 \frac{1 - [1 - 3\alpha(1 - \alpha)]^{1/2}}{1 + [1 - 3\alpha(1 - \alpha)]^{1/2}}; \quad (4.1)$$

2) for $|h + k + l| = h_3 = 3N \pm 1$ the line shift is

$$\Delta(2\theta^0) = \pm \frac{270 \sqrt{3} \cos^2 \varphi}{\pi^2 h_3} \alpha \operatorname{tg} \vartheta_0, \quad (4.2)$$

where φ is the angle between the normals to the reflecting plane and the (111) plane, on which the stacking fault is located.

The maximum broadening occurs when $\alpha = 0.5$. With further increase in α , the broadening decreases, and the position of the line approaches reflection for a perfect crystal with twin orientation ACBACB... It is also possible to obtain the values of α by the method of harmonic analysis. According to Paterson, if we consider a line consisting of one type of smeared components, the Fourier coefficients are given by the expression

$$A_n = \{[1 - 3\alpha(1 - \alpha)]^{1/2}\}^n. \quad (4.3)$$

Then $-(dA_n/dn)_{n=0} = \ln[1 - 3\alpha(1 - \alpha)]^{1/2}$ differs from zero when $\alpha \neq 0$, meaning that the influence of the stacking faults on the curve $A_n = f(n)$ is qualitatively similar to the influence of dispersion. It is also possible to determine α from the line shift, using the relation

$$\frac{B_n}{A_n} = \pm \operatorname{tg} n \left[\operatorname{arctg} \sqrt{3}(1 - 2\alpha) + \frac{2\pi}{3} \right], \quad (4.4)^*$$

which is again valid when all the components have the same intensity distribution (it should be noted that the

* $\operatorname{arctg} = \tan^{-1}$.

zero point in the calculation of the Fourier coefficients should be the Bragg angle ϑ_0). The effect of deformation faults on the diffraction pattern was considered also by Warren and Warekois.¹⁶⁵

Touching upon the influence of twin faults, Paterson²¹⁹ noted that in this case the broadening of the line should be asymmetrical. A more detailed analysis of the simultaneous influence of deformation and twin faults was considered later by Gevers²²⁰ and Wagner.²²¹ Without stopping to give the derivation, let us consider only the final results. To estimate the number of twin faults a quantity β is introduced, analogous to α for deformation faults. It is found that for small α and β the line shift is determined by relation (4.2), derived by Paterson. However, the broadening becomes somewhat different. In this case

$$-\left(\frac{dA_n}{dn}\right)_{n=0} = \frac{1}{2}(3\alpha + 2\beta), \quad (4.5)$$

or, since the coefficients are usually determined as functions of L ,

$$-\left(\frac{dA_L}{dL}\right)_{L=0} = \frac{3\alpha + 2\beta}{2d_{111}} \cos \varphi, \quad (4.6)$$

where d_{111} is the interplanar spacing for the (111) planes. It is found here that the broadening of the lines is asymmetrical, and for small α and β

$$\frac{B_n}{A_n} = \frac{\beta}{\sqrt{3}}. \quad (4.7)$$

[In this case, in the determination of the Fourier coefficients, we must take as the zero point the position of the maximum of the shifted peak; it is precisely for this reason that this equation characterizes the asymmetry of the peak, and not the shift, as in (4.4).] All these expressions are valid for one separate component.

In the case of polycrystals (or powders) we observe a superposition of all the interference lines of the hkl system, i.e., to determine α and β from the broadening and shift of the lines on the x-ray patterns it is necessary to use the averaged expressions

$$-\left(\frac{dA_L}{dL}\right)_{L=0} = \frac{3\alpha + 2\beta}{2d_{111}} j \overline{\cos \varphi}, \quad (4.8)$$

$$\overline{\Delta(2\theta^0)}_{hkl} = \overline{G} j \operatorname{tg} \vartheta_0, \quad (4.9)$$

where j — the fraction of the {hkl} planes which are subject to stacking faults

$$G = \pm \frac{270 \sqrt{3} \cos^2 \varphi}{\pi^2 h_3} = \pm 90 \sqrt{3} \frac{h_3}{\pi^2 l_3^2}. \quad (4.10)$$

Table III gives the values of j , $j \overline{\cos \varphi}$ and $j \overline{G}$ for certain planes. It is seen from this table that it is quite difficult to determine β from the asymmetrical

Table III. Values of j , $j \cdot \overline{\cos \varphi}$, and $j\bar{G}$ for various reflections¹⁶⁶

hkl	j	$j \overline{\cos \varphi}$	$j\bar{G}$
111	3/4	1/4	+3.95
200	1	$1/\sqrt{3}$	-7.90
220	1/2	$1/\sqrt{6}$	+3.95
311	1/2	$\frac{1}{2} \sqrt{3/11}$	-1.44
222	3/4	1/4	-1.98

broadening of the lines, since the asymmetry is always the result of a different shift of various components due to deformation faults. The only reflection which does not become asymmetrical as a result of deformation faults is the 200 peak, from which β should indeed be determined.

In the general case, when broadening is due both to stacking faults and to dispersion, it is found²²¹ that

$$-\left(\frac{dA_L}{dL}\right)_{L=0} = \frac{1}{\bar{D}} = \frac{1}{D_p} + \frac{3\alpha + 2\beta}{2d_{111}} \overline{\cos \varphi} \cdot j, \quad (4.11)$$

where \bar{D} is the experimentally determined ("effective") dimension of the blocks, without allowance for stacking faults, and D_p is the true dimension of the blocks. If it is considered that the broadening, analogous to the presence of small blocks and caused by stacking faults, is determined, as it were, by some fictitious (apparent) dimension

$$D_F = \frac{2d_{111}}{3\alpha + 2\beta} \frac{1}{j \overline{\cos \varphi}}, \quad (4.12)$$

then we have

$$\frac{1}{\bar{D}} = \frac{1}{D_p} + \frac{1}{D_F}. \quad (4.13)$$

Recently many researchers have used these relationships to investigate stacking faults in deformed metals and alloys. The values of α and β obtained by various authors are listed in Table IV.

It is seen that a considerable concentration of stacking faults is observed in many deformed metals and alloys (up to one fault every 20 planes), and that their number increases with decreasing deformation temperature and with increasing content of the second component in the alloys. Table IV lists also for the sake of comparison the "effective" dimensions of the blocks, experimentally obtained by the harmonic-analysis method, as well as the values calculated by formula (4.12). The experimentally-obtained block sizes are determined almost entirely by the stacking faults. This is a very important result, which indicates that the effect of stacking faults on the line broadening must be taken into account for materials of this type. However, we know of no paper in our literature in which this influence is taken into account. The faults are disregarded²²⁸ even in the case when an anisotropy is observed in the experimentally de-

Table IV. Values of α , β , \bar{D} , and D_F for metals with fcc lattice

Material and its composition	$\alpha \cdot 10^3$	$\beta \cdot 10^3$	$D_F^{(111)}, \text{ \AA}$	$\bar{D}^{(111)}, \text{ \AA}$	Literature
Cu	7				222
	4				224
	4				223
	3,3		1665	1000	226
Cu*	11.7-13,3		465	450	228
	12,5	29	180	155	221
Ni	3				223
	1,65				226
Ni*	5,5				
Ag*	10	24	170	160	227
Cu + 20% Zn	25	50	95	90	221
	25				
+ 30% Zn	25	17	70	70	221
	50	66,5	60	65	225
+ 35% Zn	39		145	128	221
	51				165
+ 8% Al	34				224
+ 7,1% Sn	34				226
Al	0	0		320	233

*Filings obtained at -196°C ; in all other cases—at 20°C .

termined block size for an alloy Cu + 13% Al. Yet the block-dimension ratio obtained in this investigation, $\bar{D}^{(111)} : \bar{D}^{(100)} : \bar{D}^{(110)} = 1 : 0.5 : 0.6$, is close to the ratio $1 : 0.43 : 0.6$ that results from the stacking faults.

How can stacking faults be produced in the fcc structure? We can imagine three methods:²²⁹

a) Shift along the close-packed plane. It is assumed that the macroscopic slip in the $[10\bar{1}]$ direction consists of zigzag motions of the atoms of the type $B \rightarrow C \rightarrow B$ (Fig. 10) alternately in $\bar{b}_2 = \frac{1}{6}a [2\bar{1}\bar{1}]$ and $\bar{b}_3 = \frac{1}{6}a [11\bar{2}]$. The slip in the \bar{b}_2 direction produces stacking faults of the type ABCACABC... Thus, if a single dislocation lying in the (111) plane is divided into two incomplete dislocations (called partial dislocations by Heydenreich and Shockley) in accordance with the reaction

$$\frac{1}{2} a [10\bar{1}] \rightarrow \frac{1}{6} a [2\bar{1}\bar{1}] + \frac{1}{6} a [11\bar{2}], \quad (4.14)$$

then a stacking-fault plate is formed between them and the slip plane. The stacking fault together with the dislocations that bind it is sometimes called a stretched dislocation.

b) Removal of one close-packed plane and filling of the resultant gap by bringing the other close-packed planes together (Fig. 13). This results in a so-called sitting (semi-attached) dislocation. In practice this

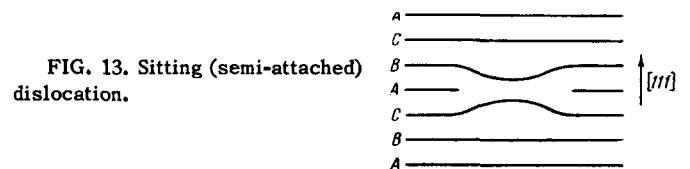


FIG. 13. Sitting (semi-attached) dislocation.

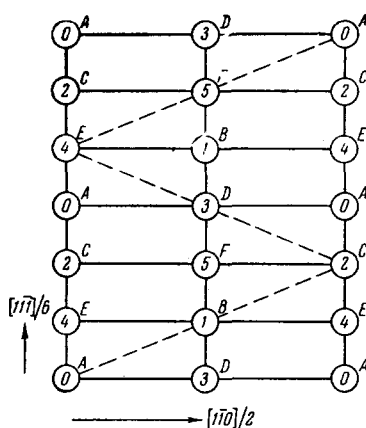


FIG. 14. Projection of the bcc structure on the (112) plane. The numbers indicate successive layers above the zero layer, and the dashed line shows their sequence in a faultless bcc structure.

can occur through a collapse of the cavity left by vacancies or by division of single dislocations, for example

$$\frac{1}{2} a [110] \rightarrow \frac{1}{3} a [111] + \frac{1}{6} a [11\bar{2}]. \quad (4.15)$$

c) Intrusion of an extra close-packed plane by settling of dislocated atoms on the (111) plane.

It follows from the foregoing mechanisms that a packing fault is more likely to occupy a certain region on the plane rather than the entire plane, as has been assumed in the calculations. It is noted in reference 224 that in the real case it is also necessary to take into account effects due to the field of stresses due to semi-dislocations, and it is assumed in this connection that the physical meaning of α is still not completely clear.

4.2. Body-Centered Cubic Lattice

In crystals with a body-centered cubic (bcc) lattice, the most important slip systems are (110)[111] and (112)[111], but only in the case of the latter can deformation or twin faults occur. The order of the stacking of the (112) plane can be written as a sequence of six layers in the form ABCDEFABCD... (Figs. 14 and 15a), and the relative shift of the layers is represented by a vector with components $\frac{1}{6} [11\bar{1}]$ and $\frac{1}{2} [1\bar{1}0]$. This sequence of layers determines the stacking order completely. A stacking fault occurs when, say, the layer D is followed again by C instead of E (Fig. 15b). Such a sequence, for example, may be due²³⁰ to the presence in the bcc lattice of a sitting dislocation formed in accordance with the reaction

$$\frac{1}{2} a [111] \rightarrow \frac{1}{3} a [112] + \frac{1}{6} a [11\bar{1}]. \quad (4.16)$$

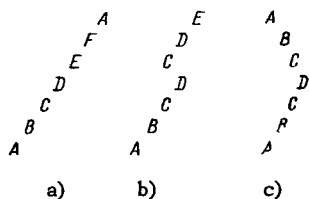


FIG. 15. Packing order of (112) planes in the bcc lattice. a) Faultless structure. b) Deformation fault. c) Twin fault.

If the stacking fault follows on each succeeding plane, a twin fault is produced (Fig. 15c).

The influence of stacking faults in the bcc structure on the position and form of the x-ray lines was considered by Hirsch and Otte²³¹ and by Guantert and Warren.¹⁶⁶ They have shown that in the case of an individual reflection from a single plane the deformation faults cause the peak to shift and spread, whereas twin faults merely spread the peak and make it asymmetrical. For polycrystals (powders) it is found, after averaging the influence of all the components, that the shift of the x-ray reflections is close to zero, and the asymmetry is too small to be noted experimentally.

However, both types of errors lead to a broadening of the reflections, depending on the indices of the plane. If we introduce the orthorhombic indices

$$H = h - k, \quad K = \frac{1}{2} h + \frac{1}{2} k + \frac{1}{2} l, \quad L_0 = -h - k + 2l, \quad (4.17)$$

then the reflections broaden when $k = 3N \pm 1$, where N is an integer, and remain sharp when $k = 3N$. For a polycrystal we have a superposition of the broadened (b) and unbroadened (u) components, so as a result we obtain an effect analogous to the effect on the broadening of dispersion with a certain fictitious dimension

$$D_F = \frac{a l_0}{1.5\alpha + \beta} \frac{\sum_b 1 + \sum_u 1}{\sum_b |L_0|}, \quad (4.18)$$

where α and β have the same meaning as before, but in the bcc lattice. The quantity $\left(\sum_b 1 + \sum_u 1\right)$ is equal to the repetition factor of the (hkl) plane in the cubic lattice. In the general case

$$-\left(\frac{dA_L}{dL}\right)_{L=0} = \frac{1}{D} = \frac{1}{D_p} + \frac{1}{D_F}. \quad (4.19)$$

Since both types of error give an analogous broadening effect, the probabilities α and β are determined not separately but only in the form of a combination $(1.5\alpha + \beta)$. The absolute and relative values of D_F for the first three reflections are listed in Table V. In addition, the authors of reference 166 have calculated the relative dimensions of the blocks in different directions under the assumption that they are bounded by parallel incoherent boundaries over the (211) or (110) planes; these dimensions are also shown in Table V.

Table V. Absolute and relative values of D_F and D_p

hkl	D_F abs	D_F rel	D_p rel boundaries over (211)	D_p rel boundaries over (110)
110	$3a/\sqrt{2}(1.5\alpha + \beta)$	2.83	1.13	0.94
200	$3a/4(1.5\alpha + \beta)$	1.00	1.00	1.00
211	$3a/\sqrt{6}(1.5\alpha + \beta)$	1.63	1.09	0.98

Table VI. Values of \bar{D}_{rel} and of $(1.5\alpha + \beta)$ for metals with bcc lattice

Material	State	\bar{D}_{rel}			$(1.5\alpha + \beta)^*$	Literature
		110	200	211		
β -brass	Filings 20°C	2.25	1	1.0	0.024	166
	after two weeks	2.26	1	1.2	0.012	
Ta	Filings-183°C	1.7	1		0.016	232
	after 1 year	1.0	1	1.0		146
W	Filings 20°C	1.0	1			187
Mo	Filings 20°C	1.0	1			
Fe	Filings 20°C	2.0	1	1.2	0.012	
	Filings-196°C	1.7	1	1.23	0.012	169

*Calculated by the broadening of the reflection from the (110) and (100) planes.

The relative values of \bar{D} and the value of $(1.5\alpha + \beta)$, obtained by various authors for different metals with bcc lattices are listed in Table VI.

In some materials the packing faults make a noticeable contribution to the line broadening. Thus, for example, in β -brass the broadening due to stacking faults is twice the broadening due to dispersion. No x-ray line shifts were noted in any of the powders of metals with bcc lattice.

5. CHANGE IN INTENSITY OF X-RAY LINES

5.1. Origin of the Notion of Distortions of the Third Kind and the First Investigations

The first to note a reduction in the integrated intensity of the higher-order reflections were Hengstenberg and Mark.²³⁴ They observed that the ratio of the intensities of the 200 and 400 reflections for different metals increase considerably (up to 40 percent) after rolling. In their opinion, this indicates a sharp weakening of

the 400 line. By plastically compressing crystals of sylvite and KCl, the same authors²³⁵ have found that after deformation the intensities of the second- and fourth-order reflections from the (100) face of the cube increased, while that of the 6th, 8th, and 10th orders decreased, and that the effect manifested itself much stronger in reflections of higher order.

Hengstenberg and Mark concluded from their experiments that the intensity of reflections is changed by distortion in the crystal lattice and that at least some of these distortions are irregular shifts of the atoms from their normal positions in the lattice. They assumed that these shifts should reduce the atomic scattering factor just as thermal motion does. Then the change in the intensity of the reflections is determined by the factor $\exp(-2M)$, where

$$M = \frac{8\pi^2}{3} \bar{u}^2 \frac{\sin^2 \theta}{\lambda^2}, \quad (5.1)$$

and \bar{u}^2 is the mean square deviation of the atoms from their ideal positions in the lattice in a direction perpendicular to the reflecting plane. These irregular displacements of the atoms were called "frozen thermal motion." In our literature they have been called distortions of the third kind.¹¹⁰

The effect of deformation on the intensity of scattering of x-rays by metals has subsequently attracted great attention on the part of researchers. Boyd,²³⁶ investigating beryllium filings, observed no reduction in the intensity of the lines compared with the annealed specimen. Brindley and Spiers,^{237,238} to the contrary, obtained a reduction in the intensity of the lines in filings of nickel, copper, and copper-beryllium alloy, compared with the intensity of the chemically prepared powders. The effect increased with increasing order of reflection. The results obtained for copper are shown in Fig. 16a (solid curve) in the form of a dependence of f'_T/f_T on $(\sin \theta)/\lambda$, where f'_T and f_T are the product of the atomic and thermal factors for filed and for chemically-prepared powders, respectively.

An analogous reduction in intensity, increasing with increasing order of reflection, was observed by Rovinskii²³⁹ for deformed copper (Fig. 16b). He assumed, however, that the experimental reduction in the intensity is not wholly an exponential function of the temperature factor, and there exists another reduction, equal for all lines; in his opinion this is also confirmed by the data of Brindley and Spiers²³⁷ (dotted curve in Fig. 16a). He advanced the hypothesis that the deformation-induced reduction in the intensity of the reflections, characterized by an exponential factor, is due not to the stable displacements of the atoms from their equilibrium position, but to an increase in the amplitudes of the thermal oscillations of the atoms in the lattice of the deformed metal (i.e., a reduction in the characteristic temperature θ). Distortions of the third kind, however, manifest themselves in an equal

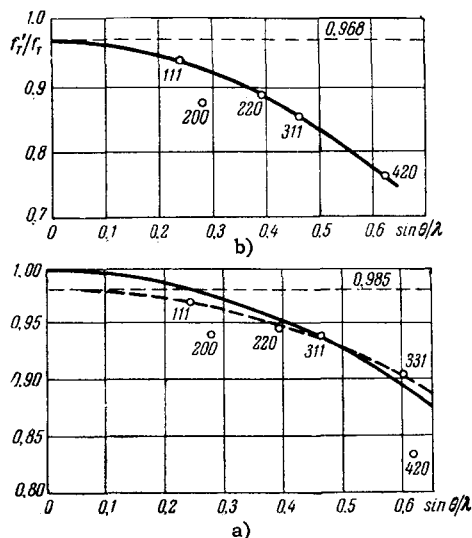


FIG. 16. Dependence of f'_T/f_T on $(\sin \theta)/\lambda$ for copper. a) From reference 237; b) from reference 239.

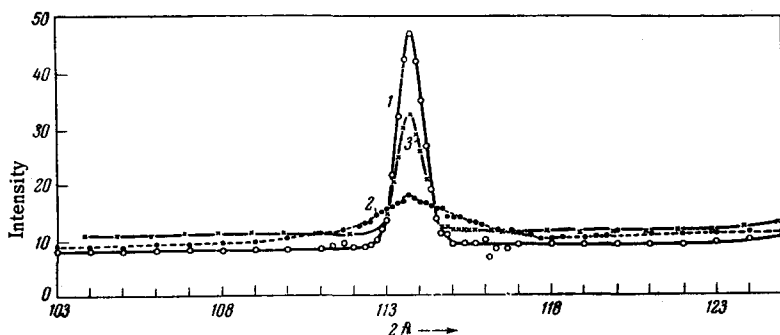


FIG. 17. The intensity of the 400 reflection of brass.²⁵³ 1 — annealed at 350°, picture taken at 25°; 2 — deformed at 25°, picture at 25°; 3 — annealed at 350°, picture at 350°.

reduction in intensity for all lines. This reduction can be explained by the fact that some of the matter is in a practically amorphous state. The anomalous behavior of the intensity of the 200 and 420 reflections (Fig. 16) have been associated by the authors of references 237 and 239 with the anisotropy of the distortions, i.e., with the unequal states of the atoms in the crystallographic planes. Later on Rovinskii²⁴⁰ proposed that such a behavior can be due to the occurrence of new coordination in the lattice. In the same work he noted that the reduction in the intensity can be due both to a reduction in θ , and to static distortions of the lattice. L. I. Vasil'ev,²⁴¹ analyzing the same problem, believed that one cannot expect any considerable change in θ through deformation.

Later on, in an investigation of rhodium, Brindley and Rindley²⁴² observed that, to the contrary, the reduction in intensity upon deformation decreases with increasing order of the reflection. Such a dependence was attributed by them to the influence of the primary extinction. The expected effect due to the lattice distortion was not noticed. In a later investigation,²⁴³ in a comparison of the earlier results,^{237,238,242} they reached the conclusion that extinction did come into play in the case of copper and nickel.

Kritskaya²⁴⁴ found the curve for the atomic factor of deformed cobalt to be lower than the calculated f -curve of the undeformed metal and to increase exponentially with the reflection angle. The atomic factor of the (010) plane had an anomalously high value.

In most of the foregoing investigations the absolute intensity was measured. A reduction in the relative intensity of reflections in strained metals was observed by Brill²⁴⁵ in iron, by Gertsriken et al.²⁴⁶ in nickel and silver, Umanskii²⁴⁷ in copper and aluminum, Il'ina et al.²⁴⁸ in iron. Boas²⁵⁰ found that the intensity of some lines of gold increased after deformation while that of others decreased, the changes not being related in any fashion with the reflection angle.

Comparing all the foregoing investigations, we can see that their results are sometimes widely divergent. But it is still unclear what causes the change in intensity in the various investigations and what is the dependence of the change on the angle of reflection. An exact interpretation is made difficult, in addition, by the large experimental errors inherent in the photo-

graphic method, and by the indeterminacy of the corrections for extinction, account of which was attempted only in reference 242.

However, the latent energy of the strained lattice as calculated from the atomic displacements obtained in the experiments agreed in order of magnitude with the energy determined by calorimetric means.^{20,251} Consequently in some later investigations particular attention was paid to an exclusion of the influence of extinction and to the accuracy of the experiments. Contributing to the latter was a new procedure for recording x-rays by means of various counters, as well as the use of monochromators.

5.2. Further Progress

a) Investigations of deformed metals in the form of powders.* Using a new technique, Hall^{252*} noted that the diffraction lines from deformed metals have "tails" that extend much further than was previously assumed. These tails are of low intensity, but since they extend over several degrees, the integrated intensity which they represent is sufficiently large. Hall considers it possible that the earlier investigators were unable to notice these tails and consequently, their values of the integrated intensity of lines of strained metals were excessively small, owing to an incorrect evaluation of the background line; the error due to this effect increases with increasing angle ϑ .

Averbach and Warren,^{253*} investigating powdered α -brass, found that the intensity of the 400 line did not change after deformation (Fig. 17), that lines with smaller reflection angle did increase in intensity, and that the intensity level of the background remained unchanged. By measuring the intensity of the lines at 350° C, they have shown that the changes due to deformation differ from changes brought about by thermal motion (see Fig. 17). In the former case the lines broaden and have very long tails, and the level of the background does not change. In the latter case the lines have much shorter tails, while the background level increases noticeably. Assuming that the increase in the intensity of the forward lines is due to a decrease in the primary extinction, the influence of which is al-

*The asterisk identifies investigations in which counters were used to register the x rays.

ready negligibly small for the 400 reflection, the authors conclude that the deformation does not change the intensity of the lines. Analogous results were obtained by Michel and Haig^{254*} in nickel. The deformation increased the intensity of the 111 and 200 lines, while the intensity of the 222 and 400 lines and the background level remained unchanged.

Wagner and Kochendorfer^{255*} measured the intensity of the background in a very large interval of angles in single crystals of zinc stretched to 32% and in polycrystals of aluminum and silver rolled to 99%. They established that the changes in the intensity do not exceed the experimental error ($\pm 10\%$).

In another investigation^{256*} in which the diffraction of neutrons by brass was investigated, it was observed that the intensity of the 111 and 200 lines remains constant, accurate to one percent. In this case the use of neutrons made it possible to avoid the influence of extinction. Nor was any change observed in the intensity of scattering of the x rays in deformed tungsten powder (0.75 percent thorium).^{146*}

Batterman,^{257*} in an investigation of iron powder in the undeformed state and after deformation in a ball grinder, established that the atomic factor of scattering is the same in both cases and agrees with the theoretical atomic factor.

Il'ina and Kritskaya,²⁵⁸ to the contrary, observed that the intensity of the x ray reflections of the 110 and 220 lines from deformed iron are weaker than the undeformed iron. The intensity of the reflections was compared with the intensity of the 111 line of copper, mixed into the iron powder. In the same investigation, and also in another one,^{259*} using hard radiation (molybdenum), which made it possible to follow the variation of the intensity with deformation of metals over a large number of reflections, the authors have concluded that their investigation has fully confirmed the existence of a variation as $\exp(-\Delta\Sigma h_1^2)$ in the attenuation of the intensity, and that the reason for the attenuation is the presence of distortions of the third kind. It should be noted that the authors have observed an increase in the determined distortions with increasing wavelength of the employed radiation.

Hall and Williamson,^{260*} in an investigation of aluminum, observed an increase in the intensity of the forward lines in deformation, while the interferences of higher indices did not change in intensity. The level of the background after deformation increased. The increase in the integral background coincided exactly with the reduction of the over-all intensity of the peak, with allowance for corrections for extinction. The over-all intensity remained constant within one percent. The authors conclude that the entire extinction is secondary. After introducing corrections for the extinction, no systematic change in the attenuation of the intensity with increasing angle ϑ has been observed; for all lines the reduction is on the average on the order of 7%.

Weiss²⁶¹ criticized the corrections for extinction which were employed before him, and derived new ones, which were reviewed and modified by Lang.²⁶² The latter used corrections in the following form: for primary extinction

$$\left(\frac{f_e}{f_T}\right)^2 = 1 - g_1 f_T^2 K_\alpha \quad (5.2)$$

for secondary extinction

$$\left(\frac{f_e}{f_T}\right)^2 = 1 - g_2 f_T^2 \frac{K_\alpha}{\sin 2\theta}, \quad (5.3)$$

where f_T is the atomic scattering factor, calculated theoretically, and f_e is the experimental value of the atomic factor, not corrected for extinction; g_1 and g_2 are the coefficients of the primary and secondary extinction, which depend on the dimensions and on the angular distribution of their blocks; K_α is a polarization factor, which has the following form for monochromatic radiation reflected from a crystal at an angle

$$K_\alpha = \frac{1 + \cos^2 2\alpha \cos^4 2\theta}{1 + \cos^2 2\alpha \cos^2 2\theta}. \quad (5.4)$$

Applying his corrections to the results of reference 260*, Lang concluded that neither of the formulas (5.2) and (5.3) justifies completely the difference between the observed and calculated intensities for copper and aluminum.

Williamson and Smallman²⁶³ considered the data of references 253* and 260* and introduced new corrections for extinction. They found that in the case of aluminum and α -brass the extinction is for the most part primary, while after deformation a decrease takes place in the intensity of the lines, on the order of $3 \pm 1\%$ for aluminum and $6 \pm 2\%$ for α -brass. The authors point out the difficulties involved in the investigation of the intensity of deformed metals, due to the strong spreading of the bases of the diffraction peaks, their possible superposition, and changes in the background.

Kochanovska²⁶⁴ proposed still another method of determining the distortions of the third kind, wherein the influence of micro-absorption is eliminated and it is possible to account — in first approximation — for the influence of primary extinction by using the Vilchinsky formula. The method is based on measurement of the intensities of three suitably chosen diffraction lines, it being assumed that the block dimensions are the same in all directions and that the reduction in the intensity of the lines of deformed metals is given by the function $\exp(-2M)$. A similar procedure was used in references 177 and 265.

Since there was no meeting of the mind regarding the nature of extinction in strained metals (while allowance for this extinction must be made if the change in intensity due to distortions in the lattice is to be evaluated), Batsur', Iveronova, and Revkevich^{266*} considered this problem in detail for powdered specimens

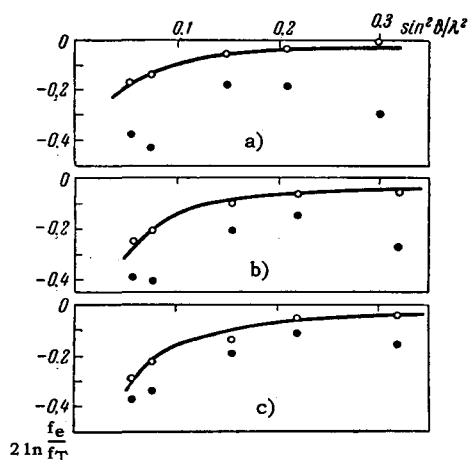


FIG. 18. The dependence of $2 \ln (f_e/f_T)$ on $\sin^2 \vartheta/\lambda^2$ (cf. reference 267). a - Copper-tin alloy; b - copper immediately after deformation; c - copper after being aged for a month at 20° .

annealed at various temperatures. Formulas (5.2) and (5.3) were used to take extinction into account. It was found that in annealing above the recrystallization temperature account must be taken of the primary extinction, and in specimens deformed or annealed at lower temperatures the secondary extinction plays the principal role.

The same authors have shown recently^{267*} that in addition to the factors already mentioned, the change in the line intensity should also be influenced by the presence of stacking faults. A crystal with one fault in the sequence of the (111) layers can be imagined as consisting of two parts, shifted relative to each other by $-\frac{1}{3}$ and $\frac{1}{3}$ along the X and Y axes, respectively (the X and Y axes are the hexagonal axes, which coincide with the directions [011] and [101] in the cubic crystal). Then the scattering intensity of such a crystal can be written in the form

$$I \approx \overline{FF^*} = F_0^2 \left[\frac{\overline{N^2}}{N^2} + \frac{\overline{(N-N_1)^2}}{N^2} + \frac{2\overline{N_1(N-N_1)}}{N^2} \cos \frac{2\pi(H-K)}{3} \right], \quad (5.5)$$

where H and K are the indices of the reflecting plane in hexagonal axes, N the total number of layers in the crystal, and N_1 the number of the "layer" in which the stacking fault took place (a "layer" is considered to be a triple group of layers forming the cell). The superior bar denotes the need for averaging over the position of the fault, i.e., over the value of N_1 . After averaging we obtain

$$T = \frac{\overline{FF^*}}{F_0^2} = \frac{2}{3} + \frac{1}{3} \cos 2\pi \left(\frac{H-K}{3} \right), \quad (5.6)$$

i.e., $T = 1$ for planes with indices $H-K = 3n$, and $T = 0.5$ for planes with indices $H-K \neq 3n$. Further, in the calculation of T_{hkl} it is considered that the reflections falling on the Debye ring come from the planes of all the groups of indices $\{hkl\}$. As a result it is found that $T_{111} = 0.62$, $T_{200} = T_{400} = 0.5$, $T_{202} = 0.75$, and $T_{311+222} = 0.72$. If the fraction of the crystals con-

taining stacking faults is α , then the intensity of the Debye ring is written in the form

$$I_{hkl} = I_{0hkl} (1 - \alpha + \alpha T). \quad (5.7)$$

It turns out in this case that even when there are few stacking faults ($\alpha = 0.2 - 0.3$), the change in the intensity is considerable.

Figure 18 shows curves of $2 \ln (f_e/f_T) = \Phi \left(\frac{\sin^2 \vartheta}{\lambda^2} \right)$ for a copper-tin alloy annealed for 10 minutes at 218° C (a), and for the two specimens of deformed copper, one immediately after deformation (b) and one aged for a month at 20° C (c). The experimental points (full circles) clearly do not fit the smooth curves. The light circles were obtained after introducing corrections for the packing faults. It is seen that the corrected experimental points fit the theoretical curves well. It is found here that $\alpha = 0.5$ for the copper-tin alloy, and 0.35 and 0.2 for copper specimens (b) and (c) respectively.

The authors of reference 267* observed no reduction in intensity due to distortions of the third kind in the copper-tin alloy. It was found, however, that in copper these distortions may or may not be observed. The result depends on the conditions of the distortion by filing, on the initial state of the material, and on its purity. In addition, aging at room temperature may lead to a complete removal of the distortions. The authors believe that in materials with low recrystallization temperature distortions of the third kind are removed at low temperatures (even room temperatures), and perhaps during the plastic deformation itself. In materials with higher recrystallization temperatures the stresses are more stable. The static shift measured in nickel is found to be on the order of 0.1 Å.

Thus, in examining the results of recent investigations it is seen that they sometimes differ quite strongly. Furthermore, different processing of the same result leads to different conclusions. The main reason for this is apparently the ambivalent allowance for extinction. First, as has already been seen, it is difficult to establish which extinction takes place, primary or secondary, and second, it is difficult to choose the correct formula for the correction. In addition, apparently, both extinctions frequently play an appreciable role simultaneously.

Generalizing the results obtained in these investigations, we can say that the intensity of x-ray lines of deformed powders* may change for many reasons, namely: 1) fragmentation of the crystals, leading to a change in extinction; 2) occurrence of distortions in the lattice, due to displacements of the atoms from the equilibrium position (distortions of the third kind); 3) occurrence of stacking faults in the layers (defor-

*If it is assumed that no preferred orientation has been produced by the preparation of the specimens.

Table VII. Ratio of intensities²⁶⁷

State of specimens	$\frac{\gamma_1}{\gamma_2} = \left(\frac{I_{400}}{I_{200}}\right)_{\text{anneal}} / \left(\frac{I_{400}}{I_{200}}\right)_{\text{def}}$	
	without correction	corrected for extinction
Deformation	1.0	1.0
Annealed at 218°, 5 hours	1.16	1.04
Annealed at 300°, 4 hours	1.16	0.98
Annealed at 400°, 4 hours	1.26	1.04

mation faults). In addition, an apparent reduction in the line intensity may be due to an incorrect drawing of the background line in an incorrect determination of the "tails" of the diffraction lines. Failure to take even one of these factors into account may lead to wrong conclusions. The importance of taking account of extinction is illustrated by the results of reference 267*. Table VII lists the ratio of the line intensities, $I_{400}/I_{200} = \gamma_1$, of annealed specimens of metals, divided by the same ratio (γ_2) for deformed specimens. The pair of lines is so chosen that the ratio of their intensities is independent of the number of packing faults. It is seen that as a result of annealing the experimentally measured ratio γ_1/γ_2 increases. If we disregard the possible effect of extinction, we can conclude that the distortions of the third kind are eliminated by annealing. However, after introducing the correction for the extinction, it is found (column 2) that the ratio remains constant. Returning in this connection to the earlier papers, considered in Sec. 5.1, we note that the analysis of the earlier results made no allowance for the possible influence of extinction (with the exception of reference 242).

There is no doubt that the question of correction for extinction has not yet been fully answered in the latest investigations. Thus, Hirsch emphasizes³ that the extinction corrections for the integrated intensity have been calculated for a crystal of infinite dimensions, the reflecting planes of which are parallel to its surface, which naturally does not take place in real crystals. As regards the Eckstein formula for primary extinction, used in references 262, 263, 266, and 267, it was obtained for the peak of the diffraction curve in scattering by a spherical particle, and not for the integrated intensity. Hirsch states that this formula can be satisfactorily used only for very small and for very large angles. In addition, further difficulties lie in the fact that any imperfections in regions whose size is comparable with the block dimension will reduce the extinction. Such imperfections may be: dislocations, disordered distributions or pile-up distributions, microdistortions, (i.e., variability in the parameter), accumulations of impurities and inclusions, groups of vacancies and submicrocracks, and stacking faults. It is still not clear whether the extinction coefficients will in this case have the same form as for the block model.

b) Change in line intensity upon deformation of solid polycrystalline specimens. Since it has been estab-

lished toward the end of the Forties that plastic deformation leads to the occurrence of distortions of the third kind, many papers have appeared in which their magnitude was related to the mechanical characteristics of the metals.^{199,249,268-274} The mean-square displacements \bar{u}^2 (distortions of the third kind) have been determined in the following manner. If the deformation causes the line intensity to change from I_0 to I , we have according to (5.1)

$$\bar{u}^2 = \frac{3}{16\pi^2} \ln \frac{I_0}{I} \frac{\lambda^2}{\sin^2 \theta}. \quad (5.8)$$

We measure here not the absolute values I_0 and I , but their ratio to the intensity of the standard or of the background. The value of \bar{u}^2 can be deduced from the change in the ratio of intensities of two lines. Then

$$\bar{u}^2 = \frac{3a^2}{4\pi^2 (\Sigma h_{i2}^2 - \Sigma h_{i1}^2)} \ln \left(\frac{I_1}{I_2} \frac{I_{02}}{I_{01}} \right), \quad (5.9)$$

where the subscripts 1 and 2 pertain to different reflections.

The use of (5.8) and (5.9) is valid only when the entire change in line intensity is due only to distortions of the third kind. However, as already noted, the intensity of the lines and their ratio are greatly influenced by extinction changes due to deformations and stacking faults. In addition, in the case of deformation of solid specimens the intensity of the lines may change also as the result of formation of a preferred orientation — texture, to which particular attention was paid in references 275 — 277. Smirnov²⁷⁷ has shown that the development of a texture may cause the intensity of the different reflections to increase, decrease, or remain unchanged. Naturally, under the joint action of texture and extinction it is very difficult to separate the change in intensity due to distortions of the third kind, particularly since the effect of the latter is apparently much less than the effect of the first two factors.^{267,277}

It follows from all the foregoing that a change in intensity of a line, taken separately, or a change in the intensity ratio of two lines, cannot characterize the distortions of the third kind unless the effects of texture, extinction, and packing faults are eliminated. Yet, in all the papers already cited,^{199,234,247,268-274*} and also in papers published after this question has been clarified,²⁷⁸⁻²⁸¹ no account is taken of either extinction or texture. In other papers,^{177,249,277,282,283} where the ratio of intensities of reflections from two orders is used,† only the influence of the texture is

*It should be emphasized that these investigations include the research of Hengstenberg and Mark,²³⁴ in which, as has been assumed, the distortions of the third kind were observed for the first time.

†This ratio is not independent of the texture for every form of deformation, nor even for every picture setup.²⁷⁵ Methods of eliminating the influence of texture for one order of reflection are discussed in references 275 and 284.

excluded. Thus, in the overwhelming majority of papers devoted to strained solid polycrystals, the conclusions concerning the magnitude of the distortions of the third kind and their variation with the degree of deformation cannot be considered as well founded. Iveronova et al.²⁶⁷ believe that many questions regarding the connection between these distortions and the change in the mechanical properties are still unanswered.

An investigation was also made of the change of intensity of x-ray reflections from crystal specimens exposed to radiations of various kinds.²⁰⁵ The results obtained are quite varied: in some cases the intensity decreases, in others it increases, and in still others it remains unchanged.

5.3. Static and Dynamic Distortions

As already noted, changes in the intensities of x-ray interferences in strained metals or alloys can be due in principle either to irregular displacements of atoms from their equilibrium position (static distortions or distortions of the third kind) or to changes in the characteristic temperature θ (dynamic distortions).

A method for separating these factors was proposed in references 248 and 285. In the general case the intensity is determined by the expression

$$I = I_0 \exp(-2M_1) \exp(-2M), \quad (5.10)$$

in which

$$M_1 = \frac{6\hbar^2}{mk\theta} \left[\frac{\Phi(x)}{x} + \frac{1}{4} \right] \frac{\sin^2 \phi}{\lambda^2}, \quad (5.11)$$

where $x = \theta/T$, Φ is the Debye function, m is the mass of the atom, while \hbar and k are the known constants. Since the first term in (5.10) depends on the temperature, and the second does not, they can be separated by taking pictures of the specimens at different temperatures, T_1 and T_2 . Then

$$\ln \frac{I_1}{I_2} = \ln \frac{I_{01}}{I_{02}} - \frac{12I^2}{mk\theta} \left[\frac{\Phi(x_1)}{x_1} - \frac{\Phi(x_2)}{x_2} \right] \frac{\sin^2 \phi}{\lambda^2}. \quad (5.12)$$

A plot of $\ln(I_1/I_2)$ vs. $(\sin^2 \phi)/\lambda^2$ results in a line whose slope yields the factor in front of $(\sin^2 \phi)/\lambda^2$, hence θ . Knowing θ we can then determine M , hence \bar{u}^2 .

И'ина et al.^{248,286} obtained data in favor of the assumption that in strained pure metals (iron or molybdenum) the lattice distortions are static. In solid solutions,^{240,285-297} both static and dynamic distortions are possible, and both forms of distortion may be changed by the deformation. With this result in mind, it should be noted that in investigations made on deformed alloys,²³⁸⁻²⁵³ the calculated intensities may not agree with the experimental ones, corrected for extinction, owing to the change in the characteristic temperature.

The aforementioned method of separation is based on the assumed validity of the Debye-Waller correc-

tion, in which the characteristic temperature is the same for all reflections. Yet there are indications^{298,299} that in this correction the rms thermal displacement of the atoms is not only a function of θ and T , but also a function of the crystallographic direction. This may introduce an error in the determination of the characteristic temperature from the ratio of the intensities of the reflections from different planes. Krivoglaz³⁰⁰ has shown recently that this method of separation is not always feasible for another reason, too. He found that a change of the static displacements \bar{u}^2 is simultaneously accompanied by a change in the amplitudes of the atomic vibrations, so that the contribution of both effects is not additive, as was considered earlier.

The change in the characteristic temperature, as determined by the method described, accompanying the formation of alloys and their deformations, is usually associated²⁸⁸⁻²⁹⁷ with the change in interatomic binding forces. In some recent papers, however, the opinion has been expressed that the Debye-Waller law is valid only for monatomic substances,³⁰¹ and that the observed change in θ is connected with a certain distribution of the location of the atoms in the solid solution,³⁰² i.e., the values of θ determined by x-ray diffraction cannot be considered in this case as a measure of the interatomic forces.

5.4. Concerning Classification of Distortions, the Structure of Deformed Metals, and the Internal Stresses Corresponding to these Distortions

The foundations for the classification of structure distortions and internal stresses were laid in references 108-111. According to this classification, all structure distortions, like the residual stresses corresponding to these distortions, were grouped into distortions of the first, second, and third kind. Later on it was decided to dispense with the term "stresses of the third kind" and only the term "distortions of the third kind" was retained, since in a volume commensurate with the volume of the elementary cell, the concept of "stress" cannot be used in the sense of the theory of elasticity, as pointed out by Sachs.³⁰³ Dehlinger¹⁹² again returned to the term "residual stresses of the third kind," assuming these stresses to be produced by the near field of the dislocations produced by plastic deformation.

Recently, in connection with many of the investigations reported in Secs. 2-5 of this review, a need arose for modifying somewhat the earlier classification. Thus, for example, the shift of the x-ray lines cannot serve as a unique criterion for the existence of only residual stresses of the first kind in a specimen, since such a displacement can result also from stresses of the second kind. Likewise, in view of the considerable improvement in the procedures for measuring intensity, it has been found that the clear cut connection previously established between the distortions of the third kind and the change in intensity of

the x-ray lines is not confirmed in many cases, so that the existing estimates of the magnitudes of the distortions of the third kind, developed in metal under plastic deformation, may prove to be too high and, in any case, call for a thorough review. By the same token, apparently, the connection between the latent deformation energy and distortions of the third kind needs re-evaluation. Summarizing the discussions on the classification, published in the journal "Zavodskaya laboratoriya" (Plant Laboratory),³⁰⁴⁻³⁰⁹ Davidenko formulated the definition of residual stresses as follows:

1. Stresses of the first kind, or macrostresses, are those which are balanced in volumes commensurate with the volume of the body and can be observed by cutting the body in parts. They appear on the x-ray photographs as shifts in the interference maxima, but the shift can be eliminated by suitably cutting the body.

2. Stresses of the second kind, or microstresses, are those balanced within volumes of the same order of magnitude as the volumes of one or several crystallites. Their x-ray diffraction manifestation is in the smearing of the interference maxima, and also in a shift (of these maxima) which cannot be eliminated by cutting.

3. Distortions of the third kind are disturbances to the regular placement of the atoms in the lattice; since their x-ray diffraction manifestation has not yet been finally established, they are not yet included in a classification by x-ray symptoms.

Like any other classification, this one is incomplete. It does not include, naturally, such structure distortions as the stacking faults described in Sec. 4 of the present survey. The possibility is not excluded that other types of structure distortions, which influence the diffraction of x-rays, will be discovered in the future.

6. DISLOCATION DATA OBTAINED BY X-RAY DIFFRACTION

6.1. Determination of Dislocation Density

a) Use of Debye-Scherrer x-ray patterns. To calculate the density of the dislocations, Williamson and Smallman³¹¹ used two quantities which can be determined by x-ray diffraction: the block dimension D and the width of the microstress distribution $\xi = 2(\Delta d/d)$. In the first case, assuming that the dislocations lie on the boundaries between the blocks, their density is determined as follows. The over-all length of the dislocation line on one block is $6nD/2$, where n is the number of dislocations on the surface of the block. Since the number of blocks per unit volume is $1/D^3$, the density of the dislocations will be

$$\rho = \frac{3n}{D^2}. \quad (6.1)$$

When using this equation, the value of n must be either determined or specified. The value $n = 1$ gives the minimum density of dislocations and can be used for annealed or very strongly deformed metals, when the distribution of the dislocations becomes almost disordered.³¹¹ As regards the block dimension D , the value of ρ is determined by the microbeam method, by measuring the primary extinction, or by the broadening of the diffraction lines and their displacement (in the latter case as the distance between the stacking faults).

The dislocation density can also be determined from the microdistortions. If we know the rms strain $\bar{\epsilon}^2$ for any distribution, then the corresponding latent energy of the lattice is

$$V = \frac{3E\bar{\epsilon}^2}{2} = \frac{3EA\xi^2}{2}, \quad (6.2)$$

where A is a coefficient that depends on the character of the distribution of the microdeformation, and its values are $1/2\pi$ and ~ 2 for Gauss and Cauchy distributions, respectively. The energy of a screw dislocation v_c in the absence of interaction with other dislocations is

$$v_c = \frac{\mu b^2}{4\pi} \ln \frac{r}{r_0}, \quad (6.3)$$

where b is the Burgers vector, r is the radius of the crystal containing the dislocation, and r_0 is a suitably chosen²³⁰ integration limit, usually on the order of 10^{-7} cm. Since the dislocations do interact, the elastic energy changes on the average by a factor F , i.e.,

$$v = v_c F. \quad (6.4)$$

Then the density of the dislocations, obtained in this manner, is

$$\rho = \frac{V}{v} = \frac{k}{F} \frac{\xi^2}{b^2}, \quad (6.5)$$

where

$$k = 6\pi EA/\mu \ln \left(\frac{r}{r_0} \right).$$

The calculation given in reference 311 yields $k = 16.1$ for fcc metals with a Burgers vector b directed along [110], and $k = 14.4$ for bcc metals with b directed along [111].

In the present case the value of F must again be determined or specified. The simplest assumption is $F = 1$. A model in which $F = 1$ approximately is a network in which a dislocation coincides with each edge of the block; then the distance between the dislocations is a maximum and the interaction is minimal. In addition, for this model we obviously have $n = 1$. A criterion of the correctness of these assumptions can be the fulfillment of the equality $\rho_p = \rho_s$, where ρ_p and ρ_s are the dislocation densities determined by Eqs. (6.1) and (6.5) under the condition $n = 1$ and $F = 1$. The values of ρ_p and ρ_s , calculated by

Table VIII. Dislocation density in metals, calculated from data on the dimensions of the particles and sizes of the microstresses³¹¹

Material and its purity	State	ρ_s ($P=1$)	D, cm		ρ_p ($n=1$)
			by extinction	by broadening of the line	
Al (99.99%)	Annealed, 500° Filings, 20°	$4.0 \cdot 10^9$	$3.5 \cdot 10^{-4}$		$2.4 \cdot 10^7$
			$2.6 \cdot 10^{-4}$		$4.5 \cdot 10^7$
Al commercial	Filings, 20° Filings, -183°	$2.4 \cdot 10^{10}$	$2 \cdot 10^{-4}$		$7 \cdot 10^7$
		$3.2 \cdot 10^{11}$	$0.7 \cdot 10^{-4}$		$6 \cdot 10^8$
Fe Armco	Annealed, 675° Filings, 20° Filings, -183°	$3.7 \cdot 10^{11}$	$1.2 \cdot 10^{-4}$	10^{-5}	$2 \cdot 10^8$
		$6.9 \cdot 10^{11}$		10^{-5}	$3 \cdot 10^{10}$ $3 \cdot 10^{10}$
Al commercial	Annealed, 1860° Filings, 20°	$5.8 \cdot 10^{11}$	$2 \cdot 10^{-4}$	10^{-5}	$7 \cdot 10^7$ $3 \cdot 10^{10}$
α -brass	Annealed, 350° Filings, 20°	$1.2-3 \cdot 10^{12}$	$1.35 \cdot 10^{-4}$	$1.2 \cdot 10^{-6*}$	$2.4 \cdot 10^8$
					$2.5 \cdot 10^{12}$

*Distance between stacking faults.

Williamson and Smallman³¹¹ from various sources, are listed in Table VIII.

In estimating the reliability of the resultant values of ρ , it is always necessary to bear in mind the indeterminacy of the experimental values of D and \bar{e}^2 (see Secs. 3.3 and 3.4), and also the fact that in the very calculation of ρ_p and ρ_s some additional assumptions are made. Williamson and Smallman³¹¹ believe that the most reliable values of D are determined from the primary extinction. Hirsch,³ however, in view of the unsatisfactory nature of the extinction corrections, doubts that this method can yield real information on the nature and degree of perfection of a well annealed metal.

b) Broadening of the rotation curve on a double crystal spectrometer. In Hirsch's opinion,³ the most reliable x ray data on the distribution of dislocations are obtained by measuring the disorientation of the blocks with a double crystal spectrometer. If a perfect crystal is rotated about its reflecting position, it reflects the x rays only within a range of several seconds. Real crystals frequently have a rotation curve of much greater angular width (on the order of several minutes). Sometimes the rotation curve consists also of several peaks, which undoubtedly is evidence of the presence of several disoriented blocks. Most frequently it represents one peak, but broader than theoretically expected.

If data on the disorientation are available, they can be used to estimate the distribution and density of the dislocations. It is known³ that if the disorientation angle on the boundary, α , is small, then the density of dislocations is determined by the expression*

*In this case the definition of the dislocation density differs from ρ in Eq. (6.1). For the case³¹¹ of an isotropic distribution of dislocations, $\rho = 3N_D$.

$$N_D = \frac{\alpha}{bD}. \quad (6.6)$$

If α is unknown, we can estimate the upper and lower limits of the dislocation density. Assuming the crystal to be bent uniformly, we have in the plane perpendicular to the flexure axis $\alpha = D\gamma/T$, where T is the width of the region bent by the observed angle γ , i.e., T is usually equal to the grain dimension or to the diameter of the illuminated area of the crystal (whichever is smaller). Then

$$N_D = \frac{\gamma}{bT}. \quad (6.7)$$

The upper limit is determined by assuming that the subcrystallites are disoriented about their central position, and their normals have a Gaussian distribution. Then³ $\alpha \sim \gamma/3$ and

$$N_D \sim \frac{\gamma}{3bD}. \quad (6.8)$$

If D is unknown, the upper limit for the case of arbitrary distribution of the dislocations is found to be³

$$N_D = \frac{\gamma^2}{9b^2}. \quad (6.9)$$

The dislocation density calculated from Eq. (6.9) is listed in Table IX, along with some other results. A comparison of the dislocation density calculated from (6.9) with the density determined by the number of etch pits for germanium, gave good agreement.³¹²

c) Systematization of data on the dislocation density. A comparison of the data on the dislocation density, determined by various methods, shows that in undeformed crystals the dislocation density lies between 10^4 and 10^8 cm^{-2} , and for the overwhelming majority of specimens, obtained by various methods, the density is greater than 10^6 cm^{-2} . As a result of deformation, the dislocation density increases to $10^8 - 10^{11}$ cm^{-2} , and depends on the type and purity of the metal, and also on the form, de-

Table IX. Limiting dislocation densities in crystals³

Crystal and its state	γ	$N_D^{\text{upper}}/\text{cm}^2$	$N_D^{\text{lower}}/\text{cm}^2$
Aluminum (99.999%), recrystallization (grain size 30μ)	3'	$3 \cdot 10^8$	$1.3 \cdot 10^7$
Aluminum (99.993%), bent and annealed	$\sim 2'$	10^8 (density inside subgrain)	$5 \cdot 10^6$
Copper (99.999%), recrystallization (grain size 30μ)	$\sim 1'$	$2 \cdot 10^7$	$4 \cdot 10^6$
NaCl, from melt	4"	$8 \cdot 10^4$	
NaCl, polished	4'	$3 \cdot 10^6$	
Fe, whiskers ³¹³		10^6	

gree, and temperature of the deformation. Annealing of deformed crystals leads to a reduction in the dislocation density. Very little is known as yet concerning the exact distribution of dislocations in either undeformed or deformed metals.

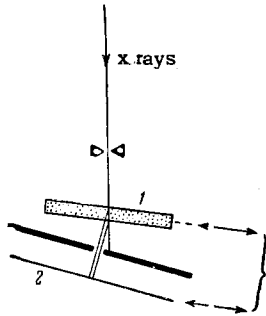


FIG. 19. Schematic diagram of the main features of Lang's method.³¹⁴
1 - crystal; 2 - film; 3 - screen.

6.2. Direct Observation of Dislocations

The foregoing methods of determining the dislocation density are no longer sensitive at densities less than 10^6 cm^{-2} . Lang, assuming that the dislocation can be detected more readily by its effect on the intensity of reflection from the surrounding region than on the angular region of reflection from a relatively large volume of the crystal, proposed a method³¹⁴ for observing individual dislocations. The principal scheme of the method is shown in Fig. 19. The primary x-ray beam, which is narrow in the plane of the figure, passes through the crystal in such a way that the Bragg reflection is from the planes that are approximately perpendicular to the surface of the crystal. The reflected rays are registered on film. The resultant pattern was called by Lang a sectional topograph. He assumes that the dislocations are observed in this case as regions of increased reflection intensity, as a result of their influence on the distribution of the energy between the multiply reflected primary and diffracted beams. In this way he obtained³¹⁵ for the dislocations in silicon 3 mm thick a pattern that agreed very well with the pattern obtained by passage of infrared rays

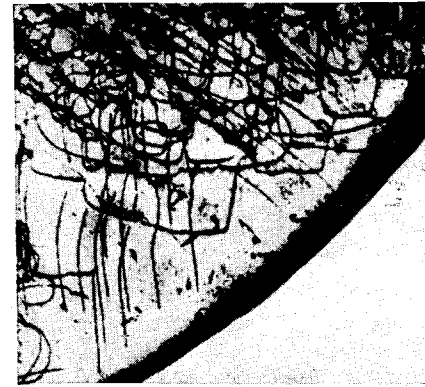


FIG. 20. Sectional topograph of dislocations in silicon obtained from the 220 reflection. The (111) planes are parallel to the surface of the flat crystal.

through the same part of the crystal after copper was deposited on the dislocations. Figure 20 shows one of the patterns obtained by Lang for silicon.³¹⁶

By determining the position of the dislocations in individual cross sections, it is possible to obtain a three-dimensional picture of their distribution. To obtain this information more rapidly, Lang³¹⁶ resorted to simultaneous displacement of the film and of the specimen parallel to their own surfaces (Fig. 19). The two-dimensional picture obtained on the film is a projection of the crystal and its imperfections. It is equivalent to a superposition of many sectional topographs and was called by Lang a projection topograph. By obtaining a pair of projection topographs (a stereoscopic pair) for reflections from the (hkl) and $(\bar{h}\bar{k}\bar{l})$ planes respectively, it was possible to determine the three-dimensional distribution of the dislocations within the volume of the crystal. This method yielded the distribution of dislocations in a whole series of a great variety of materials.³¹⁷⁻³¹⁹

Lang's procedure was used by Webb³²⁰ to study the "whiskers" of NaCl. A direct observation of the dislocations by reflection of x rays was also carried out by Bonse and Kappler^{321,322} and by Newkirk.³²³

¹ G. Greenough, *Progr. Metal. Phys.* **3**, 176 (1952).

² *Internal Stresses and Fatigue in Metals. Proceedings of the Symposium.* Ed. by G. M. Rassweiler and W. L. Grube. N. Y., Elsevier, 1959.

³ P. Hirsch, *Progr. Metal. Phys.* **6**, 236 (1956).

⁴ B. Warren, *Progr. Metal. Phys.* **8**, 147 (1959).

⁵ A. F. Ioffe and M. V. Kirpicheva, *Phil. Mag.* **43**, 204 (1922).

⁶ H. Lester and R. Aborn, *Army Ordnance* **6**, 120, 200, 283, 384 (1925).

⁷ G. I. Aksenov, *Ж. прикл. физ. (J. of Applied Phys.)* **6**, 3 (1939). *Вестн. металлпром. (Herald of the Metal Industry)*, No. 2-3, 191 (1931). *JETP* **4**, 6 (1934). *J. Tech. Phys. (U.S.S.R.)* **5**, 721 (1935).

⁸ G. Sachs and J. Weerts, *Z. Phys.* **64**, 344 (1930).

⁹ F. Wever and H. Möller, *Arch. EHW* **5**, 215 (1931).

- ¹⁰ Zheldak, Kurdyumov, and Protopopov, *Заводск. лаборатория (Plant Laboratory)* **3**, 631 (1934).
- ¹¹ H. Möller and J. Barbers, *Mitt. K.-W. Inst. Eisenforsch.* **16**, 21 (1934).
- ¹² C. Barrett and M. Gensamer, *Physics* **7**, 1 (1936).
- ¹³ R. Glocker and E. Osswald, *Z. techn. Phys.* **16**, 237 (1935).
- ¹⁴ Gisen, Glocker, and Osswald, *Z. techn. Phys.* **17**, 145 (1936).
- ¹⁵ Glocker, Hess, Schaaber, *Z. techn. Phys.* **19**, 194 (1938).
- ¹⁶ R. Glocker, *Materialprüfung mit Röntgenstrahlen*, 4 Aufl., Berlin, Springer Verlag, 1949.
- ¹⁷ M. Ya. Fuks, *op. cit. ref. 10*, **19**, 814 (1953).
- ¹⁸ D. M. Vasil'ev and Z. A. Vashchenko, *J. Tech. Phys. (U.S.S.R.)* **25**, 765 (1955).
- ¹⁹ D. M. Vasil'ev, *op. cit. ref. 10*, **25**, 70 (1959).
- ²⁰ C. S. Barrett, *Structure of Metals*, McGraw-Hill, 1943.
- ²¹ H. Möller and H. Neerfeld, *Mitt. K.-W. Inst. Eisenforsch.* **21**, 289 (1939).
- ²² H. Möller and F. Gisen, *Mitt. K.-W. Inst. Eisenforsch.* **19**, 57 (1937).
- ²³ Thum, Saul, and Peterson, *Z. Metallkunde* **31**, 352 (1939).
- ²⁴ M. M. Umanskii and M. P. Shaskol'skaya, *J. Tech. Phys. (U.S.S.R.)* **16**, 1283 (1946).
- ²⁵ A. Schaal, *Z. Metallkunde* **41**, 293 (1950).
- ²⁶ Zheldak, Kurdyumov, and Romberg, *J. Tech. Phys. (U.S.S.R.)* **7**, 1736 (1937).
- ²⁷ V. Romberg, *ibid.* **7**, 1728 (1937).
- ²⁸ D. M. Vasil'ev and S. O. Tsobkallo, *ibid.* **20**, 86 (1950).
- ²⁹ O. Schaaber, *Z. techn. Phys.* **20**, 264 (1939).
- ³⁰ W. Rachinger, *J. Scient. Instrum.* **25**, 254 (1948).
- ³¹ L. Finch, *Nature* **163**, 402 (1949).
- ³² A. Papoulis, *Rev. Scient. Instrum.* **26**, 423 (1955).
- ³³ H. Möller and J. Barbers, *Mitt. K.-W. Inst. Eisenforsch.* **17**, 157 (1935).
- ³⁴ H. Möller and G. Strunk, *Mitt. K.-W. Inst. Eisenforsch.* **19**, 305 (1937).
- ³⁵ W. Voigt, *Lehrbuch der Kristallographie*, Leipzig, 1928.
- ³⁶ B. M. Rovinskii, *op. cit. ref. 37*, **1**, 227 (1941). *Izv. Akad. Nauk SSSR, Ser. Tekhn. No. 1-2*, 87 (1942). *J. Tech. Phys. (U.S.S.R.)* **12**, 607 (1942).
- ³⁷ B. M. Rovinskii, *Инж. сб. Ин-та мех. АН СССР (Eng. Coll. Inst. Mech. Acad. Sci.)* **3**, 66 (1946).
- ³⁸ E. Macherauch and P. Müller, *Arch. EHW* **29**, 237 (1958).
- ³⁹ A. Reuss, *Z. angew. Math. und Mech.* **9**, 49 (1929).
- ⁴⁰ H. Möller and G. Martin, *Mitt. K.-W. Inst. Eisenforsch.* **21**, 261 (1939).
- ⁴¹ H. Neerfeld, *Mitt. K.-W. Inst. Eisenforsch.* **24**, 61 (1942).
- ⁴² H. Hendus and C. Wagner, *Arch. EHW* **26**, 455 (1955).
- ⁴³ J. Auld and R. Garrod, *Nature* **169**, 579 (1952).
- ⁴⁴ R. Garrod and J. Auld, *Acta Metallurgica* **3**, 190 (1955).
- ⁴⁵ V. Hauk and C. Hummel, *Z. Metallkunde* **47**, 254 (1956).
- ⁴⁶ H. Möller and H. Brasse, *Arch. EHW* **26**, 231 (1955).
- ⁴⁷ Bollenrath, Hauk, and Osswald, *Z. VDI* **83**, 129 (1939).
- ⁴⁸ F. Bollenrath and E. Osswald, *Z. VDI* **84**, 539 (1940).
- ⁴⁹ E. Heyn, *Stahl und Eisen* **37**, 470 (1917).
- ⁵⁰ R. Glocker and H. Hasenmeier, *Z. VDI* **84**, 825 (1940).
- ⁵¹ W. Wood, *Philos. Mag.* **18**, 435 (1934).
- ⁵² W. Wood, *Philos. Mag.* **19**, 219 (1935).
- ⁵³ W. Wood, *Proc. Roy. Soc.* **A172**, 231 (1939).
- ⁵⁴ B. M. Rovinskii, *JETP* **8**, 96 (1938).
- ⁵⁵ W. Wood and S. Smith, *Nature* **146**, 400 (1940).
- ⁵⁶ S. Smith and W. Wood, *Proc. Roy. Soc.* **A176**, 398 (1940).
- ⁵⁷ W. Wood and S. Smith, *Proc. Roy. Soc.* **A178**, 93 (1947).
- ⁵⁸ W. Wood and S. Smith, *J. Inst. Metals* **67**, 315 (1941).
- ⁵⁹ S. Smith and W. Wood, *Proc. Roy. Soc.* **A181**, 71 (1942).
- ⁶⁰ S. Smith and W. Wood, *Proc. Roy. Soc.* **A182**, 404 (1944).
- ⁶¹ W. Wood, *Proc. Roy. Soc.* **A192**, 218 (1948).
- ⁶² G. Greenough, *Nature* **160**, 258 (1947); *Proc. Roy. Soc.* **A197**, 556 (1949).
- ⁶³ F. Lihl, *Arch. Metallkunde* **1**, 16 (1946).
- ⁶⁴ Hauk, Möller, and Brasse, *Arch. EHW* **27**, 317 (1956).
- ⁶⁵ L. Finch, *Nature* **166**, 508 (1950).
- ⁶⁶ V. Hauk, *Naturwiss.* **40**, 507 (1953).
- ⁶⁷ G. Greenough, *J. Iron-Steel Inst.* **169**, 235 (1951).
- ⁶⁸ E. Kappler and L. Reimer, *Naturwiss.* **40**, 360 (1953); *Z. angew. Phys.* **5**, 401 (1953).
- ⁶⁹ R. Glocker and E. Macherauch, *Z. Metallkunde* **43**, 313 (1952).
- ⁷⁰ B. M. Rovinskii and T. V. Tagunova, *J. Tech. Phys. (U.S.S.R.)* **17**, 1137 (1947).
- ⁷¹ B. M. Rovinskii, *ibid.* **20**, 1497 (1950).
- ⁷² B. M. Rovinskii and N. V. Tyzhnova, *ibid.* **20**, 675 (1950).
- ⁷³ B. M. Rovinskii and V. N. Mokeeva, *Izv. Akad. Nauk SSSR, Ser. Tekhn. No. 10*, 14 (1954).
- ⁷⁴ B. M. Rovinskii and V. N. Mokeeva, *Физика металлов и металловедение (Phys. of Metals and Metallography)*, **5**, 331 (1957).
- ⁷⁵ N. N. Davidenkov and V. N. Timofeeva, *J. Tech. Phys. (U.S.S.R.)* **16**, 283 (1946).
- ⁷⁶ L. A. Glikman and V. A. Stepanov, *ibid.* **16**, 661 (1946).
- ⁷⁷ Glikman, Sanfirova, and Stepanov, *ibid.* **19**, 441 (1949).

- ⁷⁸ Davidenkov, Terminasov, and Assur, *ibid.* **19**, 1107 (1949).
- ⁷⁹ N. N. Davidenkov, *Реп. ж. Механика (Abstract Journal, Mechanics)*, No. 2, Abstr. No. 1064 (1955).
- ⁸⁰ T. Nishihara and S. Taira, *Met. Fac. Engng. Kyoto Univ.* **12**, 90 (1955).
- ⁸¹ H. Bühler, *Arch. EHW* **26**, 51 (1955).
- ⁸² C. Bateman, *Acta Metallurgica* **2**, 451 (1954).
- ⁸³ V. Hauk, *Z. Metallkunde* **46**, 33 (1955).
- ⁸⁴ D. M. Vasil'ev and A. F. Erashev, *Izv. Akad. Nauk SSSR, Ser. Fiz.* **20**, 659 (1956), *Columbia Tech. Transl.* p. 600.
- ⁸⁵ D. M. Vasil'ev, *J. Tech. Phys. (U.S.S.R.)* **26**, 2389 (1956), *Soviet Phys.-Tech. Phys.* **1**, 2310 (1957).
- ⁸⁶ B. M. Rovinskii, *J. Tech. Phys. (U.S.S.R.)* **21**, 1325 (1951).
- ⁸⁷ D. M. Vasil'ev, *ibid.* **26**, 1357 (1956), *Soviet Phys.-Tech. Phys.* **1**, 1328 (1957).
- ⁸⁸ C. Newton and H. Vacher, *J. Inst. Met.* **7**, 1193 (1956).
- ⁸⁹ Vacher, Liss, and Meds, *Acta Metallurgica* **4**, 532 (1956).
- ⁹⁰ D. M. Vasil'ev and V. A. Likhachev, *op. cit. ref. 10*, **25**, 747 (1959).
- ⁹¹ D. M. Vasil'ev, *J. Tech. Phys. (U.S.S.R.)* **28**, 2527 (1958), *Soviet Phys.-Tech. Phys.* **3**, 2315 (1959).
- ⁹² D. M. Vasil'ev, *Физика твердого тела* **1**, 1736 (1959), *Soviet Phys.-Solid State* **1**, 1586 (1960).
- ⁹³ D. M. Vasil'ev and L. V. Kozhevnikov, *ibid.* **1**, 1316 (1959), *translation* **1**, 1207 (1960).
- ⁹⁴ E. Macherauch and P. Müller, *Naturwiss.* **44**, 389 (1957).
- ⁹⁵ R. Glocker and E. Macherauch, *Naturwiss.* **44**, 532 (1957).
- ⁹⁶ C. Leiber and E. Macherauch, *Naturwiss.* **45**, 35 (1958).
- ⁹⁷ E. Macherauch, *Naturwiss.* **45**, 125 (1958).
- ⁹⁸ E. Macherauch and P. Müller, *Z. Metallkunde* **49**, 324 (1958).
- ⁹⁹ B. M. Rovinskii and V. G. Lyuttsau, *J. Tech. Phys. (U.S.S.R.)* **27**, 345 (1957), *Soviet Phys.-Tech. Phys.* **2**, 309 (1957).
- ¹⁰⁰ D. M. Vasil'ev, *Некоторые проблемы прочности твердого тела (Some Problems in the Strength of Solids)*, *Acad. Sci. Press*, 1959, p. 37.
- ¹⁰¹ B. M. Rovinskii and V. M. Sinaiskii, *Izv. Akad. Nauk SSSR, Ser. Tekhn.* **6**, 137 (1959).
- ¹⁰² B. M. Rovinskii and V. M. Sinaiskii, *op. cit. ref.* **100**, p. 49.
- ¹⁰³ D. M. Vasil'ev and G. I. Arkovenko, *Физика твердого тела* **2**, 543 (1960), *Soviet Phys.-Solid State* **2**, 507 (1960).
- ¹⁰⁴ G. I. Aksenov, *JETP* **4**, 627 (1934).
- ¹⁰⁵ A. Schaal, *Z. Metallkunde* **36**, 153 (1944).
- ¹⁰⁶ G. I. Aksenov and V. A. Moshchanskii, *Izv. Akad. Nauk SSSR, Ser. Fiz.* **21**, 226 (1957), *Columbia Tech. Transl.* p. 229.
- ¹⁰⁷ F. Brasse and H. Möller, *Arch. EHW* **29**, 757 (1958).
- ¹⁰⁸ G. Masing, *Z. techn. Phys.* **6**, 569 (1925).
- ¹⁰⁹ A. van Arkel, *Physika* **5**, 208 (1925); *Naturwiss.* **13**, 662 (1925).
- ¹¹⁰ N. N. Davidenkov, *Z. Metallkunde* **24**, 25 (1932). *Coll. Рентгенография в применении к исследованию материалов (X-ray Diffraction Applied to Research on Materials)*, ONTI, 1936.
- ¹¹¹ G. S. Zhdanov and Ya. S. Umanskii, *Рентгенография металлов (X-ray Diffraction of Metals)*, Part 2, GONTI, 1938.
- ¹¹² V. Cagliotti and G. Sachs, *Z. Phys.* **74**, 647 (1932).
- ¹¹³ F. Lihl, *Phys. Z.* **35**, 460 (1934).
- ¹¹⁴ S. Secito, *Sci. Repts. Toh. Univ.* **16**, 410 (1927).
- ¹¹⁵ U. Dehlinger, *Z. Kristallogr.* **65**, 615 (1927).
- ¹¹⁶ S. T. Konobeevskii and Y. P. Selisskii, *Phys. Z. Sowjetunion* **4**, 459 (1933).
- ¹¹⁷ A. van Arkel and W. Burgers, *Z. Phys.* **48**, 690 (1928).
- ¹¹⁸ F. Havort, *Phys. Rev.* **52**, 613 (1937).
- ¹¹⁹ W. Boas, *Z. Kristallogr.* **96**, 214 (1937).
- ¹²⁰ N. Ya. Selyakov, *Z. Physik* **31**, 439 (1925).
- ¹²¹ P. Scherrer, in book: R. Zsigmondy, *Kolloid-chemie*, 3 Aufl., 1920, p. 387.
- ¹²² B. Warren and J. Biscoe, *J. Amer. Ceram. Soc.* **21**, 49 (1938).
- ¹²³ A. Taylor, *Philos. Mag.* **31**, 339 (1941).
- ¹²⁴ Schoening, van Niekerk, and Haul, *Proc. Phys. Soc.* **B65**, 528 (1952).
- ¹²⁵ W. Wood, *Trans. Faraday Soc.* **31**, 1248 (1935); *Proc. Roy. Soc.* **A172**, 231 (1939); *Nature* **151**, 585 (1943).
- ¹²⁶ W. Wood, *Proc. Phys. Soc.* **52**, 110 (1940).
- ¹²⁷ W. Wood and W. Rachinger, *J. Inst. Metals.* **75**, 571 (1949).
- ¹²⁸ C. Smith and E. Stickley, *Phys. Rev.* **64**, 191 (1943).
- ¹²⁹ G. Williamson and W. Hall, *Acta Metallurgica* **1**, 22 (1953).
- ¹³⁰ F. Jones, *Proc. Roy. Soc.* **A166**, 16 (1938).
- ¹³¹ D. M. Vasil'ev, *J. Tech. Phys. (U.S.S.R.)* **26**, 1994 (1956), *Soviet Phys.-Tech. Phys.* **1**, 1929 (1957).
- ¹³² A. Kochendörfer, *Z. Kristallogr.* **105**, 393 (1944).
- ¹³³ L. I. Lysak, *Сб. трудов Лаб. металлофиз. АН УССР (Coll. Works, Lab. for Metal Physics, Acad. Sci. Ukr. S.S.R.)* No. 6, 40 (1955).
- ¹³⁴ R. Glocker, *Materialprüfung mit Röntgenstrahlen*, 3 Aufl., Brl., Springer Verlag, 1949.
- ¹³⁵ F. Bertaut, *Acta Crystallogr.* **5**, 117 (1952).
- ¹³⁶ E. Titchmarsh, *Introduction to the Theory of Fourier Integrals*, Oxford, 1937.
- ¹³⁷ C. Schull, *Phys. Rev.* **70**, 679 (1946).
- ¹³⁸ A. Stokes, *Proc. Phys. Soc.* **61**, 382 (1948).
- ¹³⁹ B. Ya. Pines, *Острофокусные трубки и прикладной рентгеноструктурный анализ (Sharp-Focus Tubes in Applied X-Ray Structural Analysis)*, Gostekhizdat, 1955.
- ¹⁴⁰ L. I. Lysak, *op. cit. ref. 133*, No. 5, 1954, p. 45.

- ¹⁴¹G. V. Kurdyumov and L. I. Lysak, *J. Tech. Phys. (U.S.S.R.)* **17**, 993 (1947).
- ¹⁴²B. Averbach and B. Warren, *J. Appl. Phys.* **20**, 885 (1949).
- ¹⁴³B. Warren and B. Averbach, *J. Appl. Phys.* **21**, 595 (1950).
- ¹⁴⁴B. Warren and B. Averbach, *J. Appl. Phys.* **23**, 497, 1059 (1952).
- ¹⁴⁵B. Warren and B. Averbach, *Imperfection in Nearly Perfect Crystals*, N.Y., John Wiley and Sons, 1952.
- ¹⁴⁶C. McKeehan and B. Warren, *J. Appl. Phys.* **24**, 52 (1953).
- ¹⁴⁷B. Warren, *Acta Crystallogr.* **8**, 483 (1955).
- ¹⁴⁸A. I. Kitaigorodskii, *Рентгеноструктурный анализ мелкокристаллических и аморфных тел (X-ray Structural Analysis of Microcrystalline and Amorphous Bodies)*, Gostekhizdat, 1952.
- ¹⁴⁹M. Paterson, *Philos. Mag.* **4**, 451 (1949).
- ¹⁵⁰A. Kochendörfer and U. Wolfstieg, *Z. Electrochem.* **61**, 83 (1957).
- ¹⁵¹M. Bertaut, *Compt. rend.* **228**, 492 (1949).
- ¹⁵²F. Brasse and H. Möller, *Arch. EHW* **30**, 685 (1959).
- ¹⁵³F. Schoening and J. van Niekerk, *J. Appl. Phys.* **26**, 726 (1955).
- ¹⁵⁴F. Schoening and J. van Niekerk, *Acta Metallurgica* **3**, 10 (1955).
- ¹⁵⁵B. Ya. Pines, *Doklady Akad. Nauk SSSR* **103**, 601 (1955).
- ¹⁵⁶O. N. Shvirin, *Изв. вузов, сер. физ. (News of the Colleges, Phys. Series)* **4**, 72 (1959).
- ¹⁵⁷J. Eastabrook and A. Wilson, *Proc. Phys. Soc.* **B65**, 67 (1952).
- ¹⁵⁸Garrod, Brett, and Macdonald, *Austr. J. Phys.* **7**, 77 (1954).
- ¹⁵⁹G. Williamson and R. Smallman, *Acta Crystallogr.* **7**, 574 (1954).
- ¹⁶⁰Fuks, Slonovskii, and Lupilov, *op. cit. ref. 74*, **2**, 328 (1956).
- ¹⁶¹O. V. Bogorodskii and Ya. S. Umanskii, *Izv. Akad. Nauk SSSR, Ser. Fiz.* **20**, 614 (1956), *Columbia Tech. Transl.* p. 558.
- ¹⁶²E. L. Gal'perin and Yu. S. Terminasov, *Кристаллография* **2**, 519 (1957), *Soviet Phys.-Crystallography* **2**, 515 (1958).
- ¹⁶³O. N. Shvirin and V. S. Shatin, *op. cit. ref. 156*, **1**, 128 (1959).
- ¹⁶⁴*Topics of the Fifth and Sixth All-Union Conferences on the Application of X Rays to Materials Testing*, Leningrad 1955, Acad. Sci. Press, 1958.
- ¹⁶⁵B. Warren and E. Warekois, *Acta Metallurgica* **3**, 473 (1955).
- ¹⁶⁶O. Guantert and B. Warren, *J. Appl. Phys.* **29**, 40 (1958).
- ¹⁶⁷A. G. Khachaturyan, *Кристаллография* **4**, 646 (1959), *Soviet Phys.-Crystallography* **4**, 606 (1960).
- ¹⁶⁸B. I. Smirnov, *Физика твердого тела* **1**, 1072 (1959), *Soviet Phys.-Solid State* **1**, 981 (1960).
- ¹⁶⁹C. Wagner, *Arch. EHW* **29**, 489 (1958).
- ¹⁷⁰U. Dehlinger and A. Kochendörfer, *Z. Metallkunde* **31**, 231 (1939); *Z. Kristallogr.* **101**, 134 (1939).
- ¹⁷¹M. Ya. Fuks and S. D'yachenko, *Izv. Akad. Nauk SSSR, Ser. Fiz.* **15**, 106 (1951).
- ¹⁷²B. M. Rovinskii and L. Rybakova, *Izv. Akad. Nauk SSSR Ser. Tekhn.* **10**, 1483 (1952).
- ¹⁷³B. M. Rovinskii, *Izv. Akad. Nauk SSSR Ser. Fiz.* **17**, 333 (1953).
- ¹⁷⁴B. Ya. Pines and N. G. Bereznyak, *J. Tech. Phys. (U.S.S.R.)* **24**, 329 (1954).
- ¹⁷⁵J. Andrew and H. Lee, *J. Iron-Steel Inst.* **165**, 389 (1950).
- ¹⁷⁶Golubkov, Il'ina, Kritskaya, Kurdyumov, and Perkas, *op. cit. ref. 244*, **5**, 433 (1958). *Op. cit. ref. 74*, **5**, 465 (1957).
- ¹⁷⁷L. I. Lysak and L. V. Tikhonov, *op. cit. ref. 74*, **7**, 757 (1959) and **9**, 119 (1960).
- ¹⁷⁸Kardonskii, Kurdyumov, and Perkas, *op. cit. ref. 74*, **7**, 752 (1959).
- ¹⁷⁹N. I. Sandler, *coll. Технология производства и свойства черных металлов (Technology of Production and Properties of Ferrous Metals)*, Khar'kov, vol. 2, 1956, p. 284.
- ¹⁸⁰M. Paterson, *Acta Metallurgica* **2**, 823 (1954).
- ¹⁸¹Golik, Sirenko, and Khotkevich, *op. cit. ref. 74*, **8**, 235 (1959).
- ¹⁸²G. A. Sirenko and V. I. Khotkevich, *op. cit. ref. 74*, **8**, 700 (1959).
- ¹⁸³W. Hall, *Proc. Phys. Soc.* **A62**, 741 (1949).
- ¹⁸⁴N. N. Davidenkov and B. I. Smirnov, *Izv. Akad. Nauk SSSR, Ser. Fiz.* **23**, 624 (1959), *Columbia Tech. Transl.* p. 606. *Исследования по жаропрочным сплавам (Research on Refractory Alloys)* **4**, 147 (1959).
- ¹⁸⁵O. V. Klyavin, and B. I. Smirnov, *Coll. Некоторые проблемы прочности твердого тела (Some Problems in Strength of Solids)*, Acad. Sci. Press, 1959, p. 56.
- ¹⁸⁶Kurdyumov, Perkas, and Khandros, *op. cit. ref. 74*, **7**, 747 (1959).
- ¹⁸⁷J. Despujols and B. Warren, *J. Appl. Phys.* **29**, 195 (1958).
- ¹⁸⁸B. M. Rovinskii and L. M. Rybakova, *Izv. Akad. Nauk SSSR Ser. Tekhn.* **4**, 100 (1959).
- ¹⁸⁹L. Bragg, *Nature* **149**, 511 (1942).
- ¹⁹⁰L. Bragg, *Proc. Cambr. Philos. Soc.* **45**, 125 (1949).
- ¹⁹¹B. Ya. Pines, *Лекции по структурному анализу (Lectures on Structural Analysis)*, Khar'kov, 1957.
- ¹⁹²U. Dehlinger, *Z. Metallkunde* **50**, 126 (1959).
- ¹⁹³A. Stokes and A. Wilson, *Proc. Phys. Soc.* **56**, 174 (1944); *Proc. Cambr. Philos. Soc.* **40**, 197 (1944); *Phys. Rev.* **70**, 698 (1946).
- ¹⁹⁴N. Blachman, *Phys. Rev.* **70**, 698 (1946).
- ¹⁹⁵Stokes, Pascoe, and Lipson, *Nature* **151**, 137 (1943).

- ¹⁸⁶ H. Megan and A. Stokes, *J. Inst. Metals* **71**, 279 (1945).
- ¹⁸⁷ I. M. Livshitz, *JETP* **8**, 581 (1938).
- ¹⁸⁸ V. I. Iveronova and T. P. Kostetskaya, *J. Tech. Phys. (U.S.S.R.)* **10**, 304 (1940).
- ¹⁸⁹ Yu. S. Terminasov, *ibid.* **18**, 517 (1948).
- ²⁰⁰ Yu. S. Terminasov and A. M. Toronov, *Изв. вузов, черн. мет. (News of the Colleges — Ferrous Metallurgy)* **7**, 75 (1959).
- ²⁰¹ L. A. Glikman and V. P. Tékht, *Doklady Akad. Nauk SSSR* **86**, 699 (1952), *op. cit. ref. 185*, p. 246.
- ²⁰² H. Möller and M. Hempel, *Arch. EHW* **25**, 39 (1954).
- ²⁰³ W. Wood and H. Tapsell, *Nature* **158**, 415 (1946).
- ²⁰⁴ B. M. Rovinskii and L. M. Rybakova, *Izv. Akad. Nauk SSSR, Ser. Tekhn.* **9**, 1241 (1953).
- ²⁰⁵ A. I. Zakharov, *Usp. Fiz. Nauk* **57**, 525 (1955).
- ²⁰⁶ D. Keating, *Phys. Rev.* **97**, 832 (1955).
- ²⁰⁷ G. Bacon and B. Warren, *Acta Crystallogr.* **9**, 1029 (1956).
- ²⁰⁸ R. Smallman and B. Willis, *Philos. Mag.* **2**, 1018 (1957).
- ²⁰⁹ Batenin, Il'ina, Kritskaya, and Sharov, *op. cit. ref. 74*, 7, 243 (1959).
- ²¹⁰ Terminasov, Yakhontov, and Poltavskii, *Izv. Akad. Nauk SSSR, Ser. Fiz.* **20**, 689 (1956), *Columbia Tech. Transl.* p. 629.
- ²¹¹ Petrova, Shashin, and Latsh, *op. cit. ref. 10*, **23**, 1372 (1957).
- ²¹² Yu. G. Myasnikov and Yu. S. Terminasov, *Научн. Докл. Высш. Школы (Металлургия) (Scient. Reports of the Colleges, Metallurgy)* **1**, 154 (1959).
- ²¹³ F. Lihl and H. Lawatsch, *Arch. EHW* **31**, 173 (1960).
- ²¹⁴ Gavranek, Fuks, and Bol'shutkin, *op. cit. ref. 74*, **1**, 494 (1955).
- ²¹⁵ H. Houska and B. Averbach, *Acta Crystallogr.* **11**, 139 (1958).
- ²¹⁶ F. Frank, *Philos. Mag.* **42**, 809 (1951).
- ²¹⁷ R. Green, *Phys. Rev.* **102**, 376 (1956).
- ²¹⁸ C. Barrett, *Tr. AIMME* **188**, 123 (1950); *Phys. Rev.* **81**, 311 (1951); *Imperfection in Nearly Perfect Crystals*, N.Y., John Wiley and Sons, 1952, p. 97.
- ²¹⁹ M. Paterson, *J. Appl. Phys.* **23**, 805 (1952).
- ²²⁰ R. Gevers, *Acta Crystallogr.* **7**, 337 (1954).
- ²²¹ C. Wagner, *Acta Metallurgica* **5**, 427, 477 (1957).
- ²²² G. Greenough and E. Smith, *Proc. Phys. Soc.* **B68**, 51 (1955).
- ²²³ J. Christian and J. Spreadborough, *Philos. Mag.* **1**, 1069 (1956).
- ²²⁴ J. Christian and J. Spreadborough, *Proc. Phys. Soc.* **B70**, 1151 (1957).
- ²²⁵ B. Warren and E. Warekois, *J. Appl. Phys.* **24**, 951 (1953).
- ²²⁶ R. Smallman and K. Westmacott, *Philos. Mag.* **2**, 669 (1957).
- ²²⁷ C. Wagner, *Rev. Metallurgie* **55**, 1171 (1958).
- ²²⁸ L. N. Guseva and A. A. Babaréko, *Doklady Akad. Nauk SSSR* **124**, 789 (1959), *Soviet Phys.-Doklady* **4**, 129 (1959).
- ²²⁹ W. T. Read, *Dislocations in Crystals*, New York, 1953.
- ²³⁰ A. H. Cottrell, *Dislocations and Plastic Flow in Crystals*, Oxford, 1953.
- ²³¹ P. Hirsch and H. Otte, *Acta Crystallogr.* **10**, 447 (1957).
- ²³² F. Schoening, *Acta Metallurgica* **4**, 510 (1956).
- ²³³ Ch. Wagner, *Freibergen Forschung.*, No. 35, 10 (1959).
- ²³⁴ J. Hengstenberg and H. Mark, *Naturwiss.* **17**, 443 (1929).
- ²³⁵ J. Hengstenberg and H. Mark, *Z. Phys.* **61**, 435 (1930).
- ²³⁶ J. Boyd, *Phys. Rev.* **45**, 832 (1934).
- ²³⁷ G. Brindley and F. Spiers, *Philos. Mag.* **20**, 882 (1935).
- ²³⁸ G. Brindley and F. Spiers, *Philos. Mag.* **20**, 893 (1935).
- ²³⁹ B. M. Rovinskii, *JETP* **7**, 963 (1937).
- ²⁴⁰ B. M. Rovinskii, *J. Tech. Phys. (U.S.S.R.)* **22**, 55, 63 (1952).
- ²⁴¹ L. I. Vasil'ev, *Труды Сиб. физ.-тех. ин-та (Trans. Siberian Phys.-Tech. Inst.)* No. 34, 283 (1955).
- ²⁴² G. Brindley and P. Rindley, *Proc. Phys. Soc.* **50**, 501 (1938).
- ²⁴³ G. Brindley and P. Rindley, *Proc. Phys. Soc.* **51**, 432 (1939).
- ²⁴⁴ V. K. Kritskaya, *Пробл. металловед. и физ. металлов (Problems of Metal Res. and Metal Phys.)* **3**, 297 (1952).
- ²⁴⁵ R. Brill, *Z. Phys.* **105**, 378 (1937).
- ²⁴⁶ Gertsriken, Dekhtyar, and Geller, *JETP* **8**, 1359, 1365 (1938).
- ²⁴⁷ Ya. S. Umanskii, *Тр. Минцветмет тзолота (Trans. Ministry for Nonferrous Metals and Gold)* ONTI, 1938.
- ²⁴⁸ Il'ina, Kritskaya, and Kurdyumov, *op. cit. ref. 244*, **2**, 222 (1951).
- ²⁴⁹ Il'ina, Kritskaya, and Kurdyumov, *op. cit. ref. 244*, **3**, 178 (1952).
- ²⁵⁰ W. Boas, *Z. Kristallogr.* **96**, 214 (1937).
- ²⁵¹ Fricke, Lohrmann, and Wolf, *Z. phys. Chem.* **B37**, 60 (1937).
- ²⁵² W. Hall, *J. Inst. Metals.* **77**, 601 (1950).
- ²⁵³ B. Averbach and B. Warren, *J. Appl. Phys.* **20**, 1066 (1949).
- ²⁵⁴ D. Michel and F. Haig, *Philos. Mag.* **2**, 15 (1957).
- ²⁵⁵ G. Wagner and A. Kochendörfer, *Z. Naturforsch.* **3a**, 364 (1948); *Ann. Phys.* **6**, 129 (1949).
- ²⁵⁶ Weiss, Clark, Corliss, and Hastings, *J. Appl. Phys.* **23**, 1379 (1952).
- ²⁵⁷ B. Batterman, *Phys. Rev.* **115**, 81 (1959).
- ²⁵⁸ V. A. Il'ina and V. K. Kritskaya, *Doklady Akad. Nauk SSSR*, **87**, 207 (1952). *op. cit. ref. 244*, **4**, 425 (1955).

- ²⁵⁹ П'ина, Kritskaya, and Kurdyumov, op. cit. ref. 74, 5, 379 (1957).
- ²⁶⁰ W. Hall and G. Williamson, Proc. Phys. Soc. **B64**, 937, 946 (1951).
- ²⁶¹ R. Weiss, Proc. Phys. Soc. **B65**, 553 (1952).
- ²⁶² A. Lang, Proc. Phys. Soc. **B66**, 1003 (1953).
- ²⁶³ G. Williamson and R. Smallman, Proc. Phys. Soc. **68**, 577 (1955).
- ²⁶⁴ A. Kochanovska, Czech. Phys. J. **4**, 290, 463 (1955).
- ²⁶⁵ L. V. Tikhonov, Doklady Akad. Nauk SSSR **122**, 389 (1959), Soviet Phys.-Doklady **3**, 1010 (1959).
- ²⁶⁶ Batsur', Iveronova, and Revkevich, Кристаллография **4**, 214 (1959), Soviet Phys.-Crystallography **4**, 192 (1960).
- ²⁶⁷ Batsur', Iveronova, and Revkevich, Izv. Akad. Nauk SSSR, Ser. Fiz. **23**, 591 (1959), Columbia Tech. Transl. p. 572.
- ²⁶⁸ Yu. S. Terminasov and E. B. Gasilova, Coll. Применение рентгеновских лучей к исследованию материалов (Application of X-rays to Material Testing), Mashgiz, 1949, p. 95.
- ²⁶⁹ S. O. Tsobkalo and V. V. Latsh, Izv. Akad. Nauk SSSR Ser. Fiz. **17**, 373 (1953).
- ²⁷⁰ T. N. Smirnova and Yu. S. Terminasov, ibid. **20**, 664 (1956), transl. p. 605.
- ²⁷¹ Yu. S. Terminasov and G. A. Feklistov, ibid. **20**, 695 (1956), transl. p. 634.
- ²⁷² V. M. Finkel', op. cit. ref. 74, **2**, 189 (1956).
- ²⁷³ L. I. Lysak, op. cit. ref. 133, No. 7, 3 (1956).
- ²⁷⁴ Petrova, Shashin, and Latsh, op. cit. ref. 10, **23**, 1372 (1957).
- ²⁷⁵ D. M. Vasil'ev, J. Tech. Phys. (U.S.S.R.) **26**, 695 (1956), Soviet Phys.-Tech. Phys. **1**, 671 (1957).
- ²⁷⁶ G. V. Fuks and G. V. Dobrovolskaya, Izv. Akad. Nauk SSSR, Ser. Fiz. **20**, 679 (1956), Columbia Tech. Transl. p. 620.
- ²⁷⁷ B. I. Smirnov, J. Tech. Phys. (U.S.S.R.) **27**, 218 (1957) and **28**, 2693 (1958), Soviet Phys.-Tech. Phys. **2**, 193 (1957) and **3**, 2461 (1959).
- ²⁷⁸ M. Holy, Czech. Phys. J. **8**, 108 (1958).
- ²⁷⁹ Yu. S. Terminasov and G. A. Feklistov, op. cit. ref. 212, **2**, 196 (1958).
- ²⁸⁰ Yu. S. Terminasov and A. G. Yakhontov, Metallovedenie i termicheskaya obrabotka metallor (Metal Research and Heat Treatment of Metals), Moscow, Mashgiz, **5**, 19 (1958).
- ²⁸¹ A. S. Nikonenko, op. cit. ref. 74, **7**, 699 (1959).
- ²⁸² L. S. Umanskii and D. M. Zlatoustovskii, op. cit. ref. 280, **3**, 11 (1958).
- ²⁸³ V. N. Zhdanova, Coll. Некоторые проблемы физики твердого тела (Some Problems in Solid State Physics), M., 1957.
- ²⁸⁴ V. M. Finkel', Izv. Akad. Nauk SSSR, Ser. Fiz. **23**, 611 (1959), Columbia Tech. Transl. p. 592. Op. cit. ref. 200, **3**, 73 (1959).
- ²⁸⁵ Iveronova, Kuz'mina, Futergendler, and Detlaf, Izv. Akad. Nauk SSSR, Ser. Fiz. **15**, 33 (1951).
- ²⁸⁶ V. A. П'ина and V. K. Kritskaya, op. cit. ref. 244, **4**, 399 (1955).
- ²⁸⁷ B. M. Rovinskii, JETP **8**, 84 (1938).
- ²⁸⁸ Kurdyumov, П'ина, Kritskaya, and Lysak, Izv. Akad. Nauk SSSR, Ser. Fiz. **17**, 297 (1953).
- ²⁸⁹ Kritskaya, Kurdyumov, and Stelletskaia, Doklady Akad. Nauk SSSR **98**, 63 (1954).
- ²⁹⁰ V. I. Iveronova and A. A. Katsnel'son, ibid. **99**, 391 (1954).
- ²⁹¹ Iveronova, Zvyagina, and Katsnel'son, Кристаллография **2**, 414 (1957), Soviet Phys.-Crystallography **2**, 408 (1958).
- ²⁹² Kritskaya, Kurdyumov, and Tikhonov, Doklady Akad. Nauk SSSR **102**, 271 (1955).
- ²⁹³ Kritskaya, Kurdyumov, and Stelletskaia, op. cit. ref. 244, **4**, 408 (1955).
- ²⁹⁴ П'ина, Kritskaya, Kurdyumov, and Stelletskaia, Izv. Akad. Nauk SSSR, Ser. Fiz. **20**, 723 (1956), Columbia Tech. Transl. p. 659.
- ²⁹⁵ S. M. Nikolaeva and Ya. S. Umanskii, ibid. **20**, 631 (1956), transl. p. 573.
- ²⁹⁶ N. I. Noskova and V. A. Pavlov, op. cit. ref. 74, **7**, 400 (1959).
- ²⁹⁷ Kushta, Mikhaïlyuk, and Korolyuk, op. cit. ref. 74, **7**, 299 (1959).
- ²⁹⁸ Weiss, DeMarco, Weremchuk, Corliss, and Hastings, Acta Crystallogr. **9**, 42 (1956).
- ²⁹⁹ K. Lonsdale and H. Grenville-Wells, Nature **177**, 986 (1956).
- ³⁰⁰ M. A. Krivoglaz, Кристаллография **4**, 813 (1959), Soviet Phys.-Crystallography **4**, 775 (1960).
- ³⁰¹ I. N. Frantsevich and V. S. Neshpor, Coll. Вопросы порошковой металлургии и прочности материалов (Problems in Powder Metallurgy and Strength of Materials), Kiev, Acad. Sci. Ukr.S.S.R. **5**, 49 (1958).
- ³⁰² V. I. Iveronova and A. P. Zvyagina, Физика твердого тела **2**, 118 (1960), Soviet Phys.-Solid State **2**, 108 (1960).
- ³⁰³ G. Sachs, Handb. Metallphys. **3**, 1 (1937).
- ³⁰⁴ N. N. Davidenkov, op. cit. ref. 10, **25**, 318 (1959).
- ³⁰⁵ N. P. Shchapov, op. cit. ref. 10, **25**, 1224 (1959).
- ³⁰⁶ D. M. Vasil'ev, op. cit. ref. 10, **25**, 1226 (1959).
- ³⁰⁷ B. M. Rovinskii, op. cit. ref. 10, **25**, 1228 (1959).
- ³⁰⁸ B. V. Sharov, op. cit. ref. 10, **25**, 1230 (1959).
- ³⁰⁹ V. M. Finkel' and V. F. Belorukov, op. cit. ref. 10, **26**, 859 (1960).
- ³¹⁰ N. N. Davidenkov, op. cit. ref. 10, **26**, 861 (1960).
- ³¹¹ G. Williamson and R. Smallman, Philos. Mag. **1**, 34 (1956).
- ³¹² S. Kulin and A. Kurtz, Acta Metallurgica **2**, 354 (1954).
- ³¹³ P. Gorsuch, J. Appl. Phys. **30**, 837 (1959).
- ³¹⁴ A. Lang, Acta Metallurgica **5**, 358 (1957).
- ³¹⁵ A. Lang, J. Appl. Phys. **29**, 597 (1958).
- ³¹⁶ A. Lang, Acta Crystallogr. **12**, 249 (1959).
- ³¹⁷ A. Lang, J. Appl. Phys. **30**, 1748 (1959).
- ³¹⁸ F. Frank and A. Lang, Philos. Mag. **4**, 383 (1959).

- ³¹⁹ A. Lang and G. Meyrick, *Philos. Mag.* **4**, 878 (1959).
- ³²⁰ W. Webb, *J. Appl. Phys.* **31**, 194 (1960); *Growth and Perfection of Crystals*, New York, 1938, 230.
- ³²¹ U. Bonse and E. Kappler, *Z. Naturforsch.* **13a**, 348 (1958).
- ³²² U. Bonse, *Z. Phys.* **153**, 278 (1958).
- ³²³ J. Newkirk, *Phys. Rev.* **110**, 1465 (1958).
- Supplementary Literature (added in proof)
- ¹ Iveronova, Popov, and Revkevich, Effect of Stacking Faults on Intensity of Debye Lines. *Кристаллография* **5**, 530 (1960), *Soviet Phys.-Crystallography* **5**, 509 (1961).
- ² V. I. Iveronova and A. P. Zvyagina, Characteristic Temperature, Determined by X-ray Methods. *Изв. вузов (Физика) (News of the Colleges - Physics)*, No. 6, 105 (1960).
- ³ O. N. Shvrin, Applicability of Correction Formulas for Primary and Secondary Extinction. *Кристаллография* **5**, 797 (1960), *Soviet Phys.-Crystallography* **5**, 758 (1961).
- ⁴ A. G. Khachatryan, Effect of Distribution of Mosaic Block Dimensions on the Scattering of X-rays, *ibid.* **5**, 354 (1960), transl. p. 335.
- ⁵ G. V. Kurdyumov, The Nature of the Hardened State of Metals — op. cit. ref. 280, No. 10, 22 (1960).
- ⁶ Ya. D. Vishnyakov and S. S. Gorelik, Stacking Faults in Cold-Worked Nickel and Chromium, op. cit. ref. 74, **10**, 841 (1960).
- ⁷ Ya. M. Golovchiner, Methods of Determining Stresses of the Second Kind and of Mosaic Block Dimensions, op. cit. ref. 10, **26**, 431 (1960).
- ⁸ S. Chandrasekhar, Extinction in X-ray Crystallography. — *Advances Phys.* **9**, 363 (1960).
- ⁹ S. Chandrasekhar, An Experimental Method of Correcting for Extinction in Crystals. — *Acta Crystallogr.* **13**, 588 (1960).
- ¹⁰ A. Kochendörfer and F. Trimborn, Röntgenographische Ermittlung von Gitterstörungen an Karbonyleisenpulvern. — *Arch. Eisenhüttenwes.* **31**, 497 (1960).
- ¹¹ K. Kolb and E. Macherauch, Nachweis einer makroskopischen Verfestigungsinhomogenität bei der Zugverformung reiner Nickels. — *Naturwiss* **46**, 624 (1959).
- ¹² E. Macherauch and P. Müller, Röntgenographische Untersuchung der Eigenspannung an Stahlproben. — *Arch. Eisenhüttenwes.* **31**, 555 (1960).

Translated by J. G. Adashko